IMPROVING NATIVE PRAIRIE RESTORATION MODELING FOR FLOOD REDUCTION USING PEDOTRANSFER FUNCTIONS

A Dissertation

by

CYNTHUJA PARTHEEBAN

Submitted to the Graduate and Professional School of
Texas A&M University
in partial fulfillment of the requirements for the degree of

DOCTOR OF PHILOSOPHY

Chair of Committee,	Fouad Jaber
Co-Chair of Committee,	Patricia Smith
Committee Members,	Raghavan Srinivasan
	Rebecca Bowling
Head of Department,	John Tracy

May 2022

Major Subject: Biological and Agricultural Engineering

ABSTRACT

Prairie restoration is widely viewed as beneficial because it can restore natural ecological and hydrologic function. Modeling of prairie restoration is essential to quantify the benefits of prairie lands. The accurate prediction of soil parameters is vital for model input to improve the model performance and for other soil related research studies. Pedotransfer functions (PTFs) generate the soil properties and variables needed to parameterize the soil water processes models from readily available soil information such as soil texture and soil organic matter. Native prairie soils are structurally different from disturbed non-prairie soils with the same soil texture, as native vegetation can improve soil physical properties due to soil aggregation and soil organic matter accumulation around the root system. We hypothesize that applying Rawls et al. (1998) PTF on native prairie soils underestimates the soil hydraulic conductivity (SOL_K). The accuracy of estimation of SOL_K was evaluated using nine existing PTFs against observed SOL_K at two watersheds with dominant land-use of prairie land. The results indicated none of the PTFs provided a better estimate. Currently, there is no PTF available explicitly designed for native prairie soils. This research developed a new PTF that incorporates root components (specific root length) to native prairie soils.

Stepwise multiple linear regression was used to develop an equation with measured data at Cypress Creek watershed (Waller County, TX). Cypress Creek watershed is dominated by fine sandy loam/sandy loam soil. Percentage of silt (SI), percentage of sand (SD), soil organic matter (OM), and specific root length (SRL) are the independent variables in the new equation to estimate the SOL_K. R^2 was 0.9226,

indicated 92% of the variation of SOL_K could be explained by CL, OM, SD, and SRL in the regression model. The accuracy of the new equation was successfully evaluated against measured SOL_K in the Clear Creek watershed (Cooke, Montague, Wise and Denton counties, TX). The Clear Creek watershed dominant soil consists of gravelly clay/clay. The new PTF was integrated into the SWAT model and the model performances were evaluated against observed streamflow for four watersheds with dominant land-use of prairie land. The simulation results were statistically satisfactory. The newly developed PTF can be applied to native prairie soils for the better prediction of SOL_K in modeling studies and other research studies.

DEDICATION

I dedicate this dissertation to my mother Late Sarojinidevi Gulendrarajah, my father Gulendrarajah Sundram, and my in-laws Late Selvarajah Kanagalingam and Late Sornam Selvarajah who were my inspiration to pursue my doctoral degree, my husband Partheeban Selvarajah who is the backbone for where I am today, and my kids Mathula Partheeban and Pavalan Partheeban for their understanding, tolerance, and endless love. Without my family, I would never have been able to complete my studies.

ACKNOWLEDGEMENTS

I would like to take this opportunity to first and foremost thank God, whose many blessings have made me who I am today.

It is my pleasure to thank everyone who has helped me with my research. I am forever grateful to my committee chair, Dr. Fouad Jaber to give me an opportunity to pursue my doctoral degree and for his guidance, support, patience, motivation, immense knowledge, and enthusiasm throughout my studies.

I would like to thank my co-committee chair, Dr. Patricia Smith, and my committee members, Dr. Raghavan Srinivasan, and Dr. Rebecca Bowling for their encouragement and insightful comments to complete my research. I wish to thank Dr. Jaehak Jeong for his valuable technical advice in SWAT model and Scott Frost from Clear Creek Watershed Authority for his support to do the field measurement in Clear Creek watershed. I wish to thank Dr. Sandun Fernando, Director of Graduate Programs, Department of Biological and Agricultural Engineering to hasten my application process at the critical situation. My thanks also go to my colleagues Dr. Bardia Haratmeh and Dr. Dhanesh Yeganatham for their valuable comments for my research and Nilani for sharing accommodation in College Station and my nannies Ramya Ranjith and Anitta Sureshkumar.

CONTRIBUTORS AND FUNDING SOURCES

Contributors

This work was supervised by a dissertation committee consisting of Professors Dr. Fouad Jaber, Dr. Patricia Smith, and Dr. Raghavan Srinivasan of the Department of Biological and Agricultural Engineering and Dr. Rebecca Bowling of the Department of Soil and Crop Sciences.

The measured saturated hydraulic conductivity data analyzed for Chapter 2 was provided by Harris County Flood District. All other work conducted for the dissertation was completed by the student independently.

Funding was provided in part by the Harris County Engineering Department as a subgrant to Texas Communities Watershed Program. Support for my tuition and stipend was in part provided by the Texas Commission on Environmental Quality and the US Environmental Protection Agency as I worked on the Rowlett Creek Watershed Characterization Project.

NOMENCLATURE

SOL_K	Saturated Hydraulic Conductivity
SOL_AWC	Soil Available Water Content
SOL_BD	Soil Bulk Density
NSE	Nash-Sutcliffe Efficiency
RSR	Root mean square Standard deviation Ratio
PBIAS	Percent Bias
SWAT	Soil and Water Assessment Tool
STATSGO	State Soil Geographic Database
SSURGO	Soil Survey Geographic Database
USDA	United States Department of Agriculture
EPA	Environmental Protection Agency
NRCS	natural Resources Conservation Service
NOAA	National Oceanic and Atmospheric Administration
CYC	Cypress Creek Watershed
CLC	Clear Creek Watershed
HWC	Headwaters Labette Creek watershed
NTR	North Thompson River basin watershed
UBR	Upper Big Sioux River watershed
USGS	United States Geological Survey
HRU	Hydrologic Response Unit

GAML	Green and Ampt Mein-Larson Model
SCS	Soil Conservation Service
CN	Curve Number
OV_N	Manning's "n" value for overland flow
GWQMN	Threshold depth of water in the shallow aquifer for return flow
GW_REVAP	Groundwater "revap" Coefficient
HRU_SLP	Average Slope Steepness
CH_K(1)	Effective hydraulic conductivity in tributary channel alluvium
CH_N(2)	Manning's "n" value for the main channel
CANMAX	Maximum Canopy Storage
MUKEY	Map Unit Key of soil
SAS	Statistical Analysis System
Keff	Effective hydraulic conductivity
R^2	Coefficient of determination
PTF	Pedotransfer Function
RMSE	Root Mean Squared Error
OM	Soil Organic Matter
CL	Percentage of Clay
SI	Percentage of Silt
SD	Percentage of Sand
SRL	Specific Root Length
ANN	Artificial Neural Networks

RTD	Root Tissue Density
D	Diameter of root
MLR	Multiple Linear Regression
ASTM	American Society for Testing Materials

TABLE OF CONTENTS

Page

ABSTRACT ii

DEDICATION iv

ACKNOWLEDGEMENTS v

CONTRIBUTORS AND FUNDING SOURCES vi

NOMENCLATURE vii

TABLE OF CONTENTS x

LIST OF FIGURES xiii

LIST OF TABLES xv

CHAPTER I INTRODUCTION 1

1.1 Organization of dissertation 3

CHAPTER II LITERATURE REVIEW 4

2.1 Benefits of Prairie Restoration 4
2.2 Flood Attenuation 6
2.3 Impact of soil characteristics on flow 7
2.4 Hydrological Modeling 9
2.4.1 Soil and Water Assessment Tool (SWAT) 11
2.5 Pedotransfer Functions 13
2.5.1 The input variables of pedotransfer functions 17

CHAPTER III MATERIALS AND METHODOLOGY 20

3.1 Modeling native prairie lands using SWAT 20
3.1.1 Description of study areas 20
3.1.2 Data Acquisition and Model setup 28
3.1.3 Model Calibration and Validation 31
3.2 Comparing the calibrated soil parameters with estimated soil parameters 34
3.2.1 Estimation of soil parameters 34
3.2.2 Evaluation of model performances 36

3.3 Analyzing the potential deficiency in existing pedotransfer functions applied for native prairie soils 37
3.3.1 Measurement of soil parameters 37
3.3.2 Description of PTFs used 39
3.3.3 Estimation of saturated hydraulic conductivity and evaluation of published PTFs 41
3.4 Development and evaluation of a new pedotransfer function 42
3.4.1 Description of study areas 42
3.4.2 Soil and Vegetation data 43
3.4.3 Specific root length (SRL) 48
3.4.4 Regression Analysis and development of new pedotransfer function 50
3.4.5 Evaluation and validation of the pedotransfer function 51
3.5 Evaluating the impact of newly developed pedotransfer function on the calibration of SWAT model 52
3.5.1 Description of Study Areas 52
3.5.2 Application of the newly developed pedotransfer function (PTF) 53
3.5.3 Evaluation of model performance 54

CHAPTER IV RESULTS AND DISCUSSION 55

4.1 Model calibration and validation results 55
4.2 Analysis of calibrated and estimated soil parameters 58
4.2.1 Comparison of simulations between calculated and calibrated soil parameters 61
4.3 Analyzing potential deficiency in existing pedotransfer functions 64
4.3.1 Input predictors to estimate the SOL_K 64
4.3.2 The measured SOL_K 65
4.3.3 SOL_K Estimation 67
4.4 Development and evaluation of a new pedotransfer function 71
4.4.1 Correlation Analysis 71
4.4.2 Multiple linear regression (MLR) 73
4.5 Evaluating the impact of newly developed pedotransfer function on the calibration of SWAT model 76
4.5.1 Distribution of soil hydraulic conductivity (SOL_Ks) 76
4.5.2 Model performances 77

CHAPTER V SUMMARY AND CONCLUSION 80

5.1 Summary 80
5.2 Conclusions 80
5.3 Future work 82

REFERENCES 84

APPENDIX A INPUT VARIABLES FOR REGRESSION ANALYSIS 96

APPENDIX B SATURATED SOIL HYDRAUCLIC OCNDUCTIVITY IN MM/HR FROM CALIBRATION, ESTIMATED FROM RALWS PTF, AND ESTIMATED FROM NEW PTF 98

LIST OF FIGURES

Page

Figure 2.1 Prairie regions of America (Haukos, 2014) 4

Figure 2.2 Illustration of hydrological cycle and flooding 7

Figure 3.1 Location of modelled watersheds in the Great Plains Region 21

Figure 3.2 Location of Cypress creek watershed, TX 23

Figure 3.3 Location of Clear Creek watershed, TX 24

Figure 3.4 Location of Headwaters Labette Creek Watershed, KS 25

Figure 3.5 Location of North Thompson River basin, IA 26

Figure 3.6 Location of Upper Big Sioux River Watershed, SD 28

Figure 3.7 Locations of study areas and SOL_K measurement sites: Cypress creek and Clear Creek 38

Figure 3.8 SOL_K measurement with double ring infiltrometer at Clear Creek watershed 39

Figure 3.9 Textures of soil series found in study areas (blue dots for Cypress creek and orange dots for Clear Creek). The texture triangle is based on USDA soil texture classification 44

Figure 3.10 Vegetation information and locations of SOL_K measurement sites of study area 45

Figure 4.1 Comparison of simulated streamflow by calculated and calibrated soil parameters of (a) Cypress creek watershed, (b) Clear Creek watershed, (c) Headwaters Labette creek watershed, (d) North Thompson River basin, and (e) Upper Big Sioux River basin 57

Figure 4.2 Distribution of SOL_K by calculated and calibrated methods for each watershed from left to right (1) Cypress creek watershed, (2) Clear Creek watershed, (3) Headwaters Labette creek watershed, (4) North Thompson River basin, and (5) Upper Big Sioux River basin 60

Figure 4.3 Scattered plot of observed stream flow versus simulated stream flow of (a1) CYC low flow, (a2) CYC high flow, (b1) CLC low flow, (b2) CLC

high flow, (c1) HWC low flow, (c2) HWC high flow, (d1) NTR low flow, (d2) NTR high flow, (e1) UBR low flow, and (e2) UBR high flow 63

Figure 4.4 Scattered plot of predicted and actual SOL_K in Cypress creek watershed .. 69

Figure 4.5 Scattered plot of predicted and actual SOL_K in Clear Creek watershed 70

Figure 4.6 Comparison of SOL_K from field measurement, by using newly developed PTF, and by using PTF by Rawls et al. (1998) at Clear Creek watershed..... 74

Figure 4.7 Distribution of SOL_Ks resulting from the three methods (New PTF, Rawls PTF, and Calibrated) in the HRUs for the four watersheds..... 77

LIST OF TABLES

Page

Table 2.1 List of selected existing hydrological models 10

Table 3.1 Description of study watersheds 22

Table 3.2 Time windows for model calibration and validation 31

Table 3. 3 Summary of the ratings of goodness of fit as per Moriasi et al., 2007 33

Table 3.4 Overview of selected published PTFs used for this study 40

Table 3.5 Information of soil, vegetation, and land-use of test sites at Cypress Creek watershed 46

Table 3.6 Information of soil, vegetation, and land-use of test sites at Clear Creek watershed 47

Table 3.7 Specific root length values of plants species 49

Table 3.8 Description and vegetation information of study areas 52

Table 4.1 Model performance results with rating according to Moriasi et al., 2007 58

Table 4.2 The results from statistical t-test 60

Table 4.3 Descriptive statistics of soil textural information and soil organic matter in Cypress creek watershed 64

Table 4.4 Descriptive statistics of soil textural information and soil organic matter in Clear Creek watershed 65

Table 4.5 Description of test sites and measured SOL_K in Cypress creek watershed .. 66

Table 4.6 Description of test sites and measured SOL_K in Clear Creek watershed 67

Table 4. 7 Statistical performances of nine published PTFs in terms of R2 and RMSE . 71

Table 4. 8 Pearson correlation coefficients and Pr>|r| among SOL_K, SRL, OM and soil texture (CL, SI, and SD) 72

Table 4. 9 Model performance results with rating according to Moriasi et al., 2007 78

CHAPTER I

INTRODUCTION

Prairies are one of the ecologically wealthiest landscapes on earth. However, they are now one of the most critically endangered ecosystems (Gerla et al., 2012; Samson and Knopf, 1994; Thompson, 1992). In North America, despite the numerous benefits of prairie lands, more than 99.9% of native grassland ecosystems have been lost mainly due to human development and agriculture (Samson and Knopf, 1994). The restoration of prairie lands can result in increased ecological benefits including increased infiltration (Gerla et al., 2012; Larson et al., 2017) and the potential attenuation of flooding. Modeling prairie restoration is essential to understanding the impact of land-use change and quantifying the benefits of prairie restoration in terms of flooding attenuation (Herkes et al., 2017; Kharel et al., 2016). An accurate or good estimation of inputs for the model is essential for calibration. Models without appropriate calibration and validation can result in faulty planning and implementation (Yu, 2003). Hydrological models require detailed soil characteristics as inputs. Soil water is a critical component in the generation of surface runoff (Bayabil et al., 2019). Reasonable soil parameters can be acquired from soil surveys and laboratory analysis which are expensive and limited in scale. Pedotransfer functions help obtain soil parameters values from basic soil information (e.g. soil texture, organic matter, etc.) (Bayabil et al., 2019).

Native prairie soils have specific soil characteristics compared to non-prairie soil, namely native prairie vegetation root systems that can significantly influence soil structure (Kay, 1990; Low, 1972; Mazurak and Ramig, 1962; Schwartz et al., 2003;

Udawatta et al., 2008). Prairie soils can accumulate more organic matter due to deep, extensive rooting, allowing them to hold more water in the soil (Chandrasoma et al., 2016; Fuentes et al., 2004). Furthermore, greater cation exchange capacity of organic matter can increase water and nutrient retention in prairies soils over time compared with non-prairie soils.

Current pedotransfer functions are likely insufficient to capture the unique soil hydraulic properties of prairie soils. Traditionally, PTFs use soil texture and organic matter information as an input to estimate the complex soil properties. A few studies showed improvement in the estimation by PTFs by adding additional inputs such as topography, vegetation, and salinity for site-specific application (Aimrun and Amin, 2009; Jana and Mohanty, 2011; Rezaei et al., 2016; Yao et al., 2015). Jana and Mohanty (2011) developed a PTF using remote sensing data include vegetation data (leaf area index) to predict soil moisture content. Currently, no PTFs incorporate a root component with raw soil data to estimate the soil hydraulic parameters needed to model prairie land restoration.

The main objective of this study is to develop a PTF that can effectively characterize native prairie soils. The specific objectives are 1) to model native prairie lands using SWAT and analyze the calibrated soil parameters with estimated soil parameters, 2) to analyze potential deficiencies in existing pedotransfer functions applied for native prairie soils resulting in gaps between measured and calculated soil parameters, 3) to develop and evaluate a pedotransfer function for estimating native prairie soil characteristics, and 4) to evaluate the impact of newly developed

pedotransfer function on the calibration of the SWAT model.

1.1 Organization of dissertation

This dissertation includes six chapters. Chapter I is designed to have a general introduction of the research, the existing research gap in pedotransfer function (PTF), and the research objectives. Chapter II addresses the literature review of prairie restoration, benefits, flood attenuation, soil hydraulic properties, hydrological modeling, and pedotransfer functions. Chapter III explains the materials and methodology used for all specific objectives. Chapter IV discusses the results of all the analysis and the discussion. Chapter V states the conclusions drawn from each specific objective and the overall conclusion from the research.

CHAPTER II

LITERATURE REVIEW

2.1 Benefits of Prairie Restoration

Prairie restoration is widely viewed as beneficial because it restores the natural ecological and hydrological functions back. In North America, native prairies are the largest vegetative province. They are found in the central part of the North American continent (Figure 2.1). Since European settlement, more than 99.9% of native prairie lands have been destroyed due to human development and agriculture (Samson and Knopf, 1994).

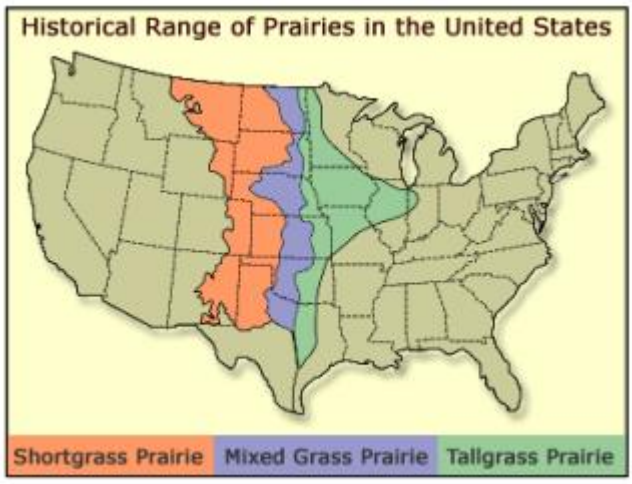

Figure 2.1 Prairie regions of America. Reprinted from [The Tallgrass Prairie History by Haukos] (Haukos, 2014)

A long list of benefits of prairie restorations includes providing habitats for wildlife, birds, and other native species, increased biodiversity, increased carbon sequestration, improvement of water quality, and flood attenuation (Cowdery et al., 2019).

Species extinction on native prairie land is a serious concern . The herbivores in native prairie land influence the nutrient cycling and soil formation. The population of dominant herbivores such as bison and prairie dogs declined due to the competition with cattle for forage, and the prevalence of diseases (Samson and Knopf, 1994). The native bird species declined due the loss of grassland habitats and the introduction of woody plants that provides habitat for non-native bird species (Samson and Knopf, 1994). Restoration of prairie land provides habitats for wildlife, space to breed native birds, and nourishment for insects.

Prairie grasslands are superior carbon sinks compare to forests with similar environmental conditions (Burke et al., 1989; Samson and Knopf, 1994). Conversion of cultivated land into grassland restores soil organic matter, which influences decomposition, soil structural improvement, and global warming (Purakayastha et al., 2008; Samson and Knopf, 1994).

Studies showed a significant reduction in nutrients such as nitrate, ammonia, nitrite, and phosphorus in groundwater and surface water at post-restoration of prairie land compared to pre-restoration (Cowdery et al., 2019).

Flood attenuation is one of the major benefits of prairie restoration (Kharel et al., 2016) and the reason for the increasing public attention for the prairie restoration (Herkes et al., 2017).

2.2 Flood Attenuation

Flooding is one of the significant disasters that affect human life drastically (Berz et al., 2001). Commonly flooding can be controlled by installing rock beams, rock ripraps, dams, sandbags, drainage, maintenance of vegetation slope, channel modification, stormwater detention, bypass channel construction, levee, and grasslands (Harris County Flood Control Disrict, 2021). Among the several strategies to attenuate flooding, restoring prairie lands has become increasingly important and widespread. Implementing a nature-based flood attention strategy is essential for an effective solution because of the price of constructing complex infrastructure (Herkes et al., 2017).

In the hydrologic cycle, flooding is one of the last stages (Figure 2.2). Prairie restorations control floods through impacting the hydrological cycle. It substantially reduced surface runoff and ditch flows during storms where the rainfall-runoff process begins. An extensive rooting system of prairies creates soil aggregates resulting in increased saturated hydraulic conductivity, which primarily depends on soil structure and influences infiltration rate and volume (Rosenzweig et al., 2016; Udawatta et al., 2008). Enhancement of infiltration rate and volume reduces surface runoff. As a result, flooding can be attenuated. Prairie soils are covered by various grasses ranging from shortgrass to tallgrass species. Grass cover retains the soil moisture and produces more organic matter due to deep, extensive rooting, allowing them to hold more water in the soil (Bharati et al., 2002; Brye and Riley, 2009; Chandrasoma et al., 2016; Fuentes et al., 2004; Rawls et al., 2003). Increasing the retention capacity of soil moisture stores more floodwater and reduces the surface runoff (Hernandez-Santana et al., 2013).

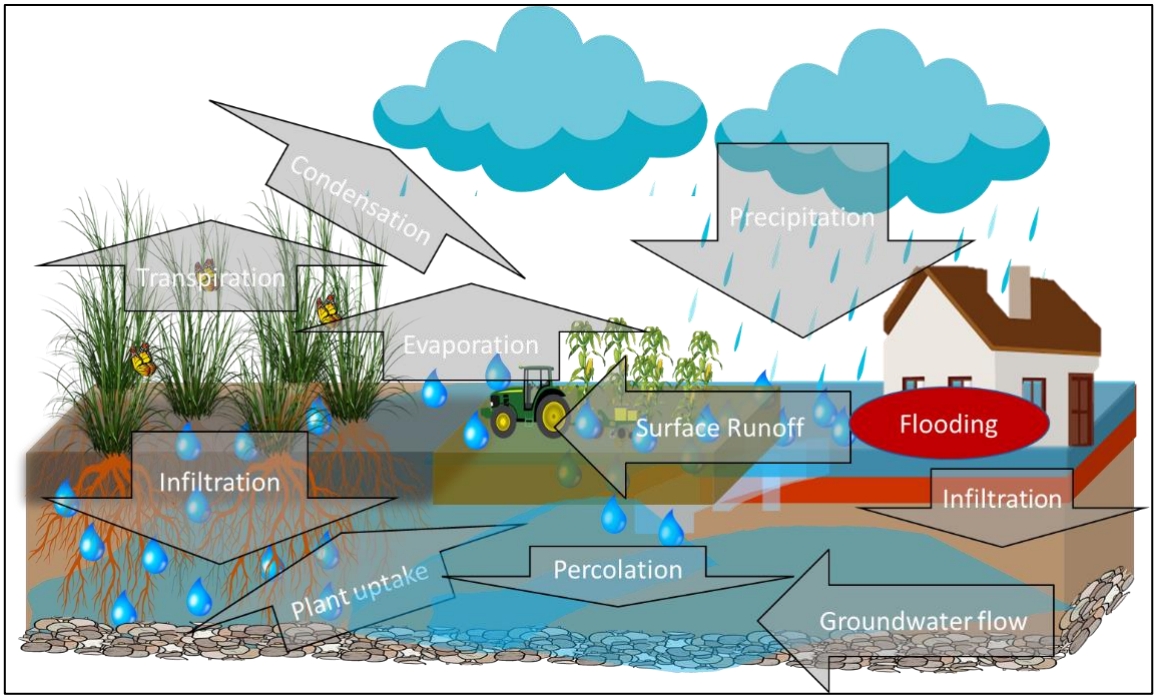

Figure 2.2 Illustration of hydrological cycle and flooding

2.3 Impact of soil characteristics on flow

An imbalance in soil water could causes flooding. Flooding occurs when runoff exceeds the infiltration in a given amount of time (Guo et al., 2014). Soil's water movement depends on its structure and texture. Soil texture is the relative proportions of sand, silt, or clay in the soil (Hillel, 2003). Well aggregated structured soil can allow downward movement of excess water in soil macropores, hold sufficient available moisture for plants, and keep enough pore space for root growth. Sandy soils have excellent aeration and drainage but a low capacity for holding water and nutrients for plant growth. A clayey soil has poor aeration and internal drainage ability. Silt has intermediate characteristics. The textural class loam implies relatively equal proportions

of sand, silt, and clay which can be the good draining ability withholding water for plant use (Kirkham, 2005).

Saturated hydraulic conductivity (SOL_K) is a crucial characteristic of soil, describing the water flow rate and pathways of water movement, partitioning precipitation into the surface runoff, and infiltration (Blanco-Canqui et al., 2017). The factors affecting the SOL_K in the natural field are cracks, root holes, wormholes, and the stability of soil crumbs. Soil texture usually has a minor effect on hydraulic conductivity, except disturbed soil materials. The hydraulic conductivity of natural soils in place varies from about 30 m/day for a silty clay loam to 0.05 m/day for clay (Kirkham, 2005).

Native prairie soils have been shown to have higher SOL_K due to their root characteristics, soil microorganisms, especially Acidobacteria and Verrucomicrobia, and richness of soil organic matter (Fuentes et al., 2004; Kalam et al., 2020; Udawatta et al., 2008). As a long-term effect, prairie soil changes to reflect the plant community growing on it (Weaver, 1961). Mechanical binding of prairie vegetation root system creates air-dry soil aggregates and produces higher soil organic matter (Chandrasoma et al., 2016; Fuentes et al., 2004; Weaver, 1958, 1961). These structural changes influence the soil's hydraulic properties. Studies showed that native prairies increase soil hydraulic conductivity and decrease soil bulk density (Chandrasoma et al., 2016; Fuentes et al., 2004; Mazurak and Ramig, 1962). To understand soil structural changes during the restoration and quantify its benefits, prairie restoration needs to be modelled using appropriate hydrological models (Herkes et al., 2017; Yang et al., 2010).

2.4 Hydrological Modeling

Hydrological models are essential tools to plan and implement new water resource management practices. Those models mathematically represent the processes involved in the hydrological cycle at the watershed scale (Yu, 2003). Hydrological models require proper procedures of identification of model, parametrization, model calibration, validation, and uncertainty assessment. An accurate or good estimation of inputs for the model is essential for calibration. Models without appropriate calibration and validation can result in faulty planning and implementation (Yu, 2003). The model performances are evaluated using statistical methods such as the Nash-Sutcliffe efficiency (NSE), Root Mean Squared Error (RMSE) – observations standard deviation ratio (RSR), and Percent Bias (PBIAS) (Moriasi et al., 2007). NSE shows how well the observed versus simulated data plots fits the 1:1 line. The model performs better when NSE approaches 1. RSR is one of the error-index statistics to evaluate the model performance. RSR varies from zero to a large positive value. Zero value indicates perfect model simulation. PBIAS indicates the average tendency of the simulated data to be larger or smaller than the respected, observed values.

Because of the nature of environmental predictions, there is no single best model. Therefore, a wide variety of different hydrologic models exist to select based on the purpose (Table 2.1). The hydrological models use parameters to represent the spatial unit (e.g., watershed) as a whole. The primary issue is the lack of adequate data to

describe the hydrological processes in the models accurately. Remote sensing provides spatially and temporally high-resolution digital form data for modeling. Geographic information systems (GIS) can be used to store, analyze, and manipulate a large number of model parameters (Singh, 1995).

Table 2.1 summarizes the existing hydrological models to simulate the hydrological process, water quality, and crops. Among those models, the Soil and Water Assessment Tool (SWAT) is one of the several widely used models for hydrological studies at the watershed scale (Arnold et al., 2012a).

Table 2.1 List of selected existing hydrological models

Model	Description	Provider	Source
HEC-HMS	Designed to simulate the complete hydrologic processes of dendritic watershed systems	US Army Corps of Engineers	(Scharffenberg, 2016)
Mike-SHE	Physics-based models for overland flow, unsaturated flow, groundwater flow, and fully dynamic channel flow, including all their complex feedbacks and interactions	Danish Hydraulic Institute (DHI)	(H. Jaber and Shukla, 2012)
ADAPT	Simulate the quantity and quality of flows associated with water table management systems; Integration of	FABE, OSU	(H. Gowda et al., 2012)

	the GLEAMS model with DRAINMOD		
DRAINMOD	Simulates the hydrology of poorly drained and artificially drained soils	BAEN, NCSU	(W. Skaggs et al., 2012)
EPIC and APEX	Simulates land management impacts for small-medium watersheds, impacts of soil erosion, and approximately eighty cops	USDA-NRCS and Texas A&M AgriLife	(Wang et al., 2012)
SWAT	Simulates hydrological processes, fate and transport of sediments and pollutants within a basin	Texas A&M University	(Arnold et al., 2012a)

2.4.1 Soil and Water Assessment Tool (SWAT)

The SWAT model is a direct extension of the SWRRB (Simulator for Water Resources in Rural Basins) model. It is a continuous, process-based, semi-distributed (lumped) model developed to quantify the impact of land management practices on water, sediment, and agricultural chemical yields in large complex watersheds with varying soils, land use, and management conditions over long periods. It simulates hydrological processes, fate, and transport of sediments and pollutants within a basin. The major model components include weather, hydrology, soil properties, plant growth, nutrients and sediment loading, microorganisms, and land management (W. Gassman et al., 2007). SWAT requires weather data of daily precipitation, maximum and minimum temperature, solar radiation, relative humidity, and windspeed.

SWAT divides a watershed into sub-watersheds further divided into hydrologic response units (HRUs). HRUs are nonspatial units, consist of similar land use, soil type, and slope within a given subbasin. Water balance is the driving force behind all the processes in SWAT. The equation of water balance is represented as below:

$$\mathrm{SWt} = \mathrm{SWo} + \sum_{i=1}^{t}(\mathrm{Rday} - \mathrm{Qsurf} - \mathrm{Et} - \mathrm{Wseep} - \mathrm{Qgw}) \quad (1)$$

where SWt is the total soil water content, SWo is the initial soil water content for a given day I (mm H2O), and Rday, Qsurf, Et, Wseep, and Qgw are precipitation, surface flow, ET, return flow, and percolation (mm H2O) respectively (Arnold et al., 2012a).

Water on the soil surface will infiltrate into the soil profile or flow on the surface as runoff during the hydrological process. The generation surface runoff can be estimated using two methods available in SWAT: Modified SCS curve number and Green and Ampt Mein-Larson Model (GAML). In the curve number method, the curve number (CN) varies non-linearly with the moisture content of the soil. The curve number drops when soil is in wilting point and increases to near 100 when soil is in saturation. GAML model requires high temporal data resolution. Here infiltration is calculated as a function of wetting front matric potential and effective hydraulic conductivity. Water does not infiltrate, flow as surface runoff. The effective hydraulic conductivity (SOL_Ke) is approximately equivalent to one-half the saturated hydraulic conductivity of the soil (Neitsch et al., 2009). The relationship between SOL_Ke and curve number is given by following equation:

$$SOL_{Ke} = \frac{56.82 x SOL\_K^{0.286}}{1+0.051 x e^{(0.062 x CN)}} - 2 \quad (2)(\text{Nearing et al., 1996})$$

This relationship explains curve number becomes sensitive to streamflow while calibrating the SWAT model even GAML option was selected to estimate the surface runoff.

2.5 Pedotransfer Functions

Pedotransfer functions (PTFs) are mathematical equations that generate the soil properties and variables needed to parameterize the soil water processes models from readily available soil information such as soil texture (Van Looy et al., 2017). PTFs add the values to basic soil properties by translating them into complex soil properties which can be laborious and expensive to determine. Briggs et al (1912) predicted a soil property from other soil properties first (Briggs and Shantz, 1912). Following that, number of studies predicted soil properties from another (Ahuja et al., 1985; van Genuchten, 1980). Then the equations for these relationships were named as "pedotransfer functions" (Bouma, 1989).

In recent years, pedotransfer functions (PTFs) have become increasingly needed for high- resolution soil parameter estimation in modeling studies to address soil and water management issues in environmental systems and understanding the impacts of climate and land-use changes. Since measuring soil hydraulic parameters with spatially high resolution is often expensive and inaccessible, those parameters need to be estimated from readily available soil information such as soil texture and soil organic matter, which can be obtained from soil surveys. PTFs translate the raw soil information into useful soil information that cannot be easily available (Bouma, 1989). The

relationship between raw soil information and complex soil hydraulic characteristics must be adequately accurate, and the range of applicability is known for the accurate description and prediction of soil processes (Pachepsky and Rawls, 1999; Patil and Singh, 2016). Soil water is a critical component in the generation of surface runoff, which leads to flooding. Soil hydraulic characteristics such as saturated hydraulic conductivity (SOL_K), soil available water content (SOL_AWC), and soil bulk density (SOL_BD) are key soil parameters for assessing the soil process. Those parameters are needed to be estimated from PTFs for hydraulic modeling studies (Bayabil et al., 2019). SOL_K is the most critical soil parameter in modeling studies. Other studies developed several pedotransfer functions to classify the SOL_K according to USDA soil textural classes (Ahuja et al., 1985; Clapp and Hornberger, 1978; Rawls et al., 1982). Based on these previous studies, Rawls et al., (1998) redefined a pedotransfer function for SOL_K according to USDA soil textural classes and two bulk density classes. Rawls et al. 1998 pedotransfer is used to estimate the SOL_K and SOL_AWC to compare to calibrated values for this study. SOL_AWC is the difference between field capacity and permanent wilting point. It is estimated by subtracting soil moisture content at -1500 kPa from the soil moisture at -33 kPa (Arnold et al., 2012a). SOL_AWC depends on soil organic matter and soil texture, where the organic matter in the soil influences the soil water retention. Soil organic matter strongly influences the field capacity compared to permanent wilting point (Rawls et al., 2003). SOL_BD is another important soil parameter to determine the soil quality (Murphy et al., 2009) and a significant input for hydrological modeling (Lenhart et al., 2002; Malone et al., 2015). Several efforts have

been done to develop pedotransfer functions to predict the bulk density of soil correlated with soil organic carbon/matter and soil texture (Adams, 1973; Alexander, 1980; Curtis and Post, 1964; Huntington et al., 1989; Rawls, 1983). Studies showed that soil parameters obtained from pedotransfer functions are commonly used in hydrological modeling (Bayabil et al., 2019; Huf Dos Reis et al., 2018; Ranjitkumar et al., 2015; Sun et al., 2016). Sun et al., 2016 estimated the soil hydraulic properties from an existing pedotransfer function with basic soil information of soil texture and soil organic matter and incorporating the parameters into SWAT simulation. Their proposed method was evaluated with a case study consisting of a watershed with general soil characteristics.

PTFs can be applicable to any soil (Kätterer et al., 2006); however, their accuracy seems to be high when ensembled or are site-specific (Cornelis et al., 2001; Pachepsky and Rawls, 1999; Yao et al., 2015). In recent years, several studies attempted to enhance the existing PTFs by adding supplementary variables such as topography and vegetation (leaf area index) (Jana and Mohanty, 2011; Leij et al., 2004; Obi et al., 2014; Pachepsky et al., 2001; Sharma et al., 2006). Additionally, several studies have been done to develop new PTFs for specific land uses (Kätterer et al., 2006; Qiao et al., 2018; Yao et al., 2015).

PTFs can be developed using various mathematical methods. Most PTFs were derived through multiple regression methods due to their simplicity (Van Looy et al., 2017; Wösten et al., 2001). Multiple regression is a model of relationship between two or more explanatory variables and a response variable by fitting an equation to observed data. Regression technique can be a linear or nonlinear regression based on the expected

relationship between variables. The accuracy and reliability of a given PTF approach is determined by how well the explanatory variables such as soil texture explain the response variable such as soil hydraulic properties. In the regression technique, the major drawback is the need for adequate prior knowledge of the relationship between inputs and outputs (Van Looy et al., 2017). Using a training dataset, the pattern of underlying relationship between input and output can be recognized and the regression technique can be applied. If there is no prior knowledge of model concept, the Artificial neural network approach (ANN) is another popular tool to build PTFs (Schaap et al., 1998; Tamari et al., 1996; Twarakavi et al., 2009; Wösten et al., 2001). ANN is a classical pattern recognition paradigm inspired by the way biological nervous systems, such as the brain, process information (Twarakavi et al., 2009). Like the structure of the human brain, the ANN models consist of neurons in a complex and nonlinear form. The neurons are connected to each other by weighted links. All the processes in ANN models, such as data collection and analysis, network structure design, number of hidden layers, network simulation, and weights/bias trade-off, are computed through learning and training methods. Although some studies showed that ANN performs better than the regression method, it has an issue of overfitting the model (Van Looy et al., 2017). A study showed no significant difference between regression method and ANN (Merdun et al., 2006). Merdun et al, (2006) developed PTF for soil ware retention and hydraulic conductivity using ANN and multiple linear regression. The predictive capabilities of two methods were compared. The predictive results differences between methods were not statistically significant.

2.5.1 The input variables of pedotransfer functions

Soil texture is widely used as a major input in PTFs to predict soil hydraulic properties. Soil texture is the relative proportions of sand, silt, and clay content. The soil texture is associated with soil porosity, which controls the water holding capacity and downward water movement. Application of detailed particle size distribution on PTF in addition to soil textural class increases the accuracy of prediction (Schaap et al., 1998).

In addition to soil texture, soil organic carbon and bulk density are the predictors commonly used in many PTFs (Ahuja et al., 1985; Rawls et al., 1998; Schaap et al., 1998; Wösten et al., 2001). Soil organic matter is the portion of soil that comprises plant and animal debris which are in different states of decomposition (Coleman et al., 1989). Studies showed that incorporating soil organic carbon increases the accuracy of results in PTFs (Rawls, 1983; Tamari et al., 1996; Wösten et al., 1999). The relationship between organic matter and SOL_K is not consistent. Even though soil organic matter enhances SOL_K, at some extent, studies show that overall, there is a negative correlation between organic matter and SOL_K (Nemes et al., 2005; Rawls et al., 2004).

The bulk density of soil refers the mass or weight of a certain volume of soil. Soil bulk density determines the infiltration, available water capacity, soil porosity, rooting depth/restrictions, soil microorganism activity, root proliferation, and nutrient availability (Fuentes et al., 2004). Aina and Periaswamy (1985) estimated available water holding capacity using predictors of sand content and bulk density. Following that study, several developed PTFs used bulk density as one of the input variables to estimate

the soil hydraulic properties (Rawls et al., 1998; Teepe et al., 2003). PTFs are available to estimate the soil bulk density using other easily available soil properties (Adams, 1973; Alexander, 1980; Curtis and Post, 1964; Kätterer et al., 2006).

Additional input variables are used in PTFs to enhance prediction (Schaap et al., 1998; Sharma et al., 2006). Studies examined the variable of topography to predict the soil hydraulic properties through PTFs (Leij et al., 2004; Pachepsky et al., 2001; Sharma et al., 2006). The results of their studies showed improvement in PTF prediction when including topographical attributes of slope, elevation, curvature, aspect, and solar radiation. Sharma et al, 2006 incorporated the vegetation attribute leaf area index in addition to topographic attributes (DEM) to estimate the soil hydraulic properties and the study suggested that inclusion of a vegetation factor enhance the prediction of variability of soil hydraulic properties.

Studies showed that native prairies have increased soil hydraulic conductivity and decreased soil bulk density (Chandrasoma et al., 2016; Fuentes et al., 2004; Mazurak and Ramig, 1962). Including root components information in PTFs is essential in calculating native prairie soil characteristics (Weaver, 1920). A study reviewed the influence of root components on soil hydraulic properties and showed that the impact on SOL_K depends on root size, root density, soil texture, and type of vegetation (Lu et al., 2020). The development of the plant's root system show high level of plasticity in response to heterogeneity of the soil (Ostonen et al., 2007). Thus, integrating the length and weight of root systems could enhance the estimation of hydraulic properties of soil. Specific root length is one the commonly used morphological parameters to represent

the root characteristics that indicate the soil heterogeneity (Leuschner et al., 2004). which means Specific root length is defined as the root length per unit root dry mass (Pang et al., 2010).

There is a research gap between existing PTFs and the native prairie soil hydraulic characteristics. We hypothesized that estimating soil hydraulic conductivity of native prairie soil with existing PTF with general predictors of soil texture and organic matter gives an inaccurate prediction. This will lead to mismanagement of native prairie conservation and misleading modeling of native prairie restoration. The research finding of this study will aim to bridge this gap. The incorporation of prairie root characteristics should enhance the predictive capability of PTF.

CHAPTER III

MATERIALS AND METHODOLOGY

3.1 Modeling native prairie lands using SWAT

3.1.1 Description of study areas

The Great Plains are one of the 15 broad level 1 ecological regions of North America (EPA, 2021). In the USA, areas of 10 states (Montana, North Dakota, South Dakota, Wyoming, Nebraska, Kansas, Colorado, Oklahoma, Texas, and New Mexico) are within the Great Plains proper. The grassland of the Great Plains contributes to the largest biome in North America (Samson and Knopf, 1994). The extreme weather (extreme cold and extreme warm)with episodic precipitation favors grass growth more over trees in this region (Lauenroth et al., 2014). Five watersheds with dominant land use of prairie land were chosen across the Great Plains in the USA from different hydroclimatic and geographic settings (Figure 3.1 and Table 3.1).

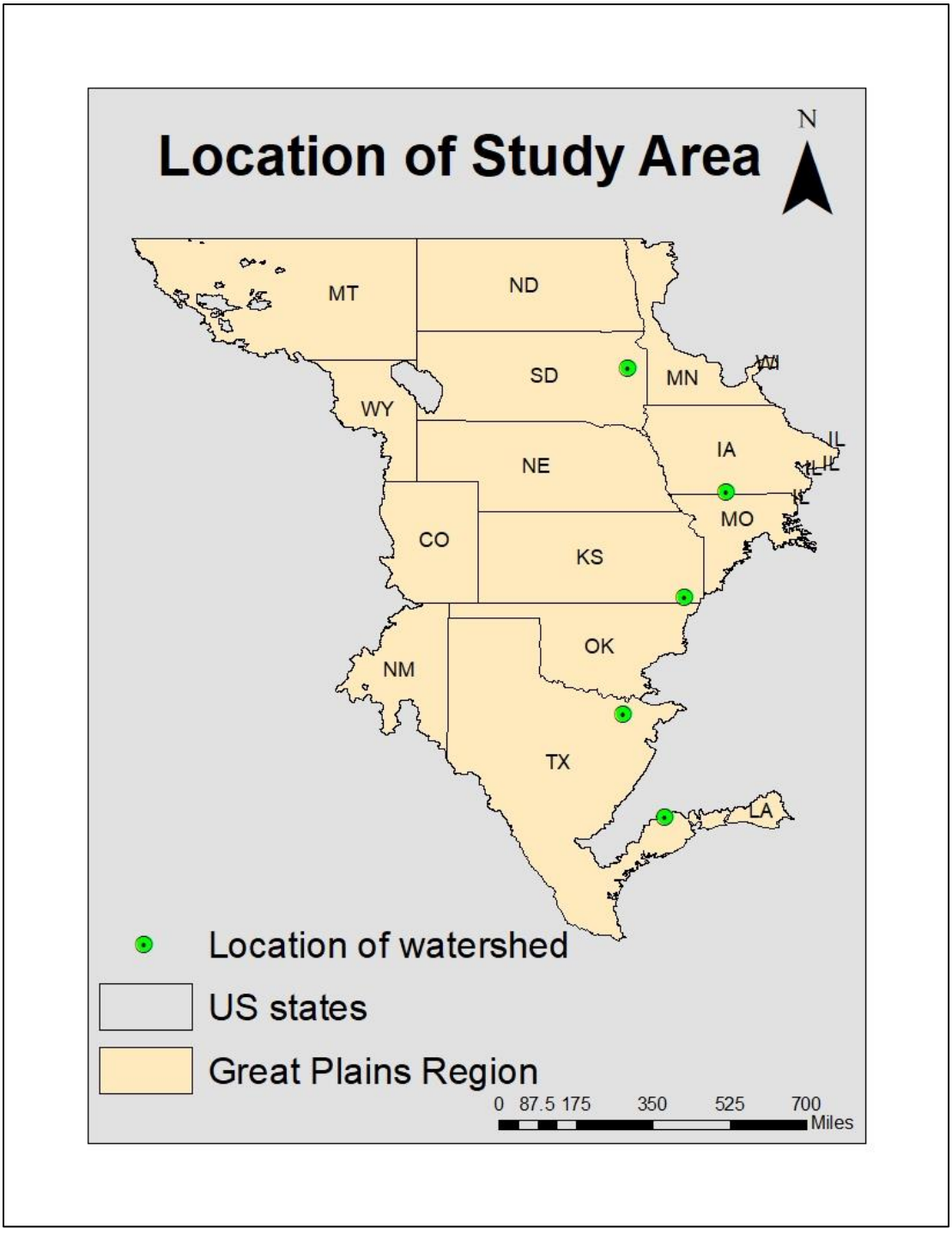

Figure 3.1 Location of modelled watersheds in the Great Plains Region

Table 3.1 Description of study watersheds

Watershed	Location	Drainage Area (sq. km)	Dominant Land Use	Dominant Soil
Cypress Creek Watershed, TX (CYC)	29°58'24.8" N and 95°35'54.79"W	333	Grassland	Fine sandy loam - Sandy clay loam
Clear Creek Watershed, TX (CLC)	33°20'10.41"N and 97°10'46.05"W	766	Grassland	Gravelly clay loam and clay
Headwaters Labette Creek Watershed, KS (HWC)	37°11'37.66" and 95°11'32.99"	554	Grassland and cropland	Silt loam – silty clay
North Thompson River Basin Watershed, IA (NTR)	40°38'25.00"N and 93°48'29.80"W	1799	Grassland and cropland	Clay loam - clay
Upper Big Sioux River Watershed, SD (UBR)	44°43'53.87"N and 97°2'40.24"W	3931	Cropland and Grassland	Loam – clay loam

3.1.1.1 Cypress Creek Watershed (CYC), TX

The Cypress Creek watershed is located in the Western Gulf Coastal plain in Texas. It lies in Harris County and Waller County. The study area has a surface area of 333 sq Km. A USGS measuring gauge 08068740 Cypress Creek at House-Hahl Road near Cypress, TX, TX (29º58’24.8”N and 95º35’54.79”W) located nearby the outlet of Little Cypress Creek was used for calibration and validation in this study (Figure 3.2).

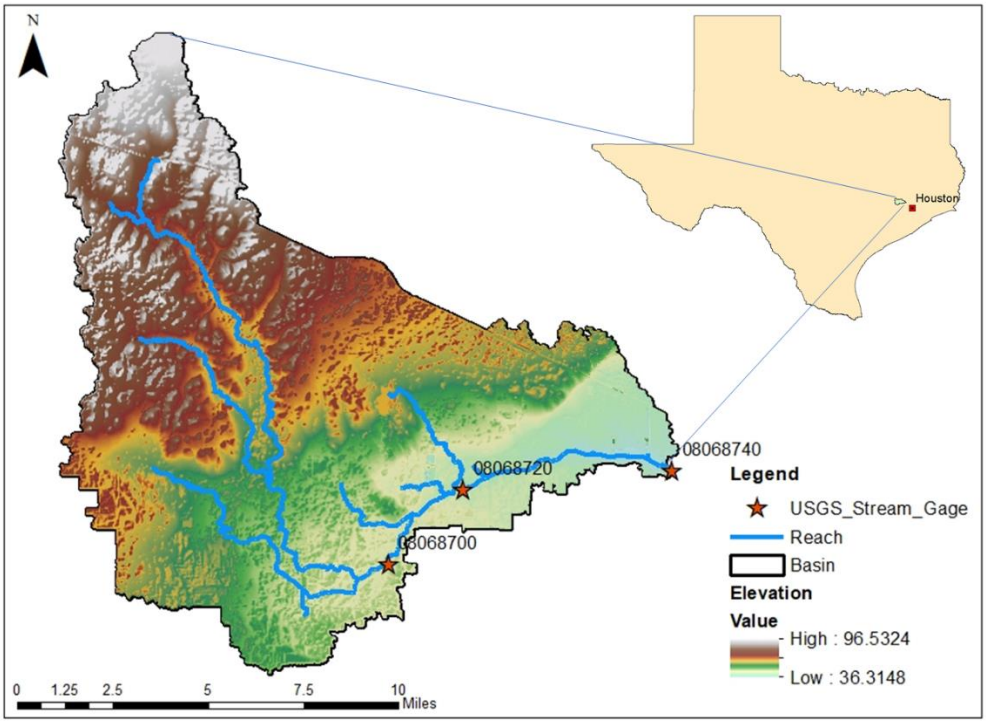

Figure 3.2 Location of Cypress Creek watershed, TX

The study area includes soil series of Katy, Hockley, Wockley, Aris, and Gessner. The dominant soil taxonomic class is sandy clay loam. On an annual basis, the average precipitation is 53 inches in Harris County (Harris County Flood Control Disrict, 2021).

3.1.1.2 Clear Creek Watershed, TX (CLC)

Clear Creek begins the central portion of the eastern part of Montague County, Texas, and flows for about 80 km into Garza-Little Elm Reservoir. This study area, Clear Creek Watershed of the Trinity River Watershed includes Blocker Creek – Clear Creek Watershed (HUC 1203010305) and part of Duck Creek – Clear Creek Watershed (HUC 1203010306). It lies in Denton, Wise, Cooke, and Montague counties, Texas. The watershed has an area of 766 sq Km (Figure 3.3).

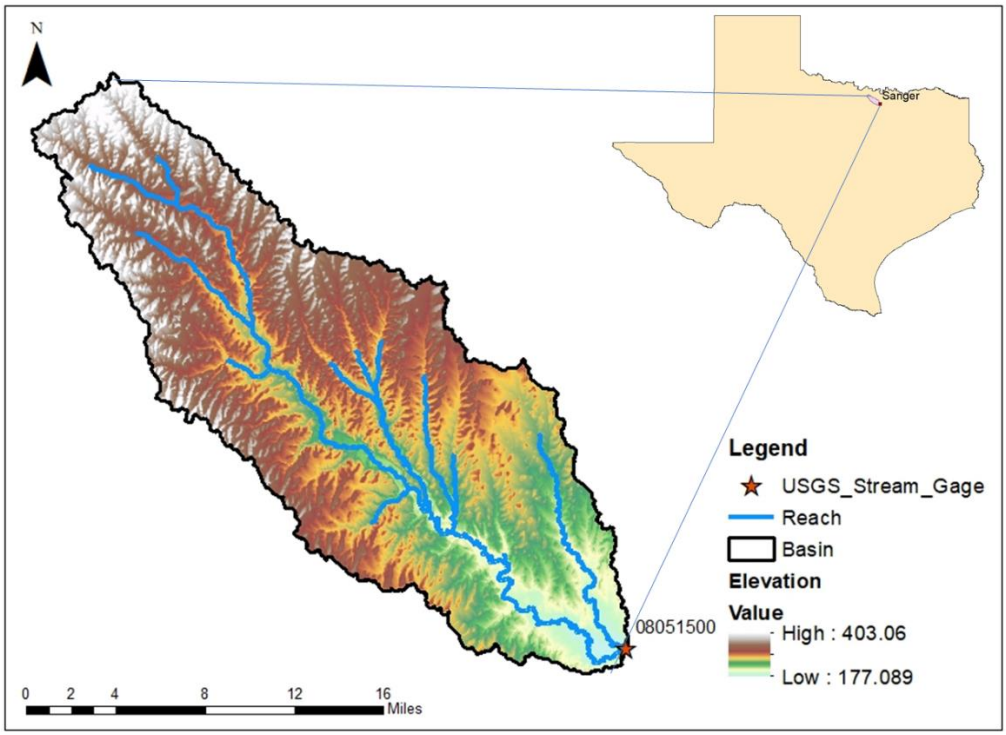

Figure 3.3 Location of Clear Creek watershed, TX

This watershed's most dominant land use is forest and grass/pastureland, which covers about 95% of the land area, and the rest is cropland. About 0.01 % of the land is a low-density residential area. The study area includes soil series of Eddy, Sanger, Gaddy,

Windthorst, Bolar, Medlin, Hensley, Bosque, and Venus. The dominant soil is gravelly clay loam and clay. The downstream area is dominated by clay loam.

3.1.1.3 Headwaters Labette Creek Watershed, KS (HWC)

This study area includes Headwaters Labette Creek Watershed (HUC 1107020504) and part of Outlet Labette Creek Watershed (HUC 1107020505). It lies within Neosho and Labette counties in Kansas. The watershed has an area of 554.46 sq km (Figure 3.4).

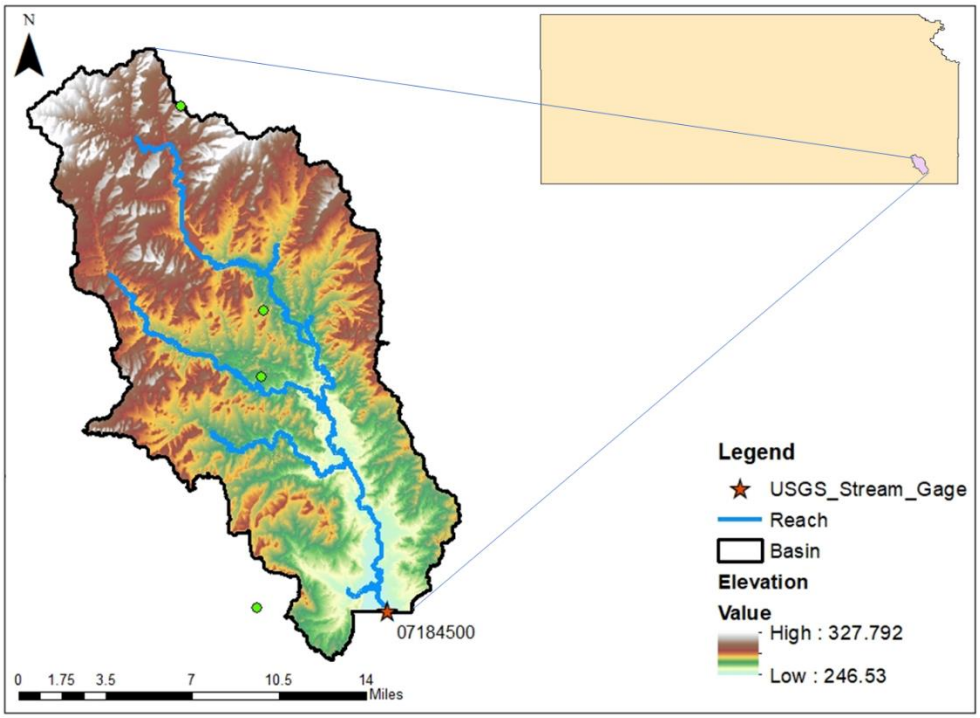

Figure 3.4 Location of Headwaters Labette Creek Watershed, KS

Most of the watershed is grassland (60% of the area), cropland (38% of the area), and the rest is impervious area. Grassland and cropland appear to be evenly distributed

across the watershed. The watershed is dominated by soil series of Cherokee and taxonomic class of fine, mixed, active, thermic Typic Albaqualfs.

3.1.1.4 North Thompson River Basin Watershed, IA (NTR)

The Thompson River initially begins east in Adair County, Iowa, into Missouri. It is the largest tributary of the Grand River in Iowa. The study area, which includes the north part of the Thompson River basin, lies in Adair, Madison, Union, Clarke, Ringgold, and Decatur counties, IA. It has an area of 1799 sq km (Figure 3.5).

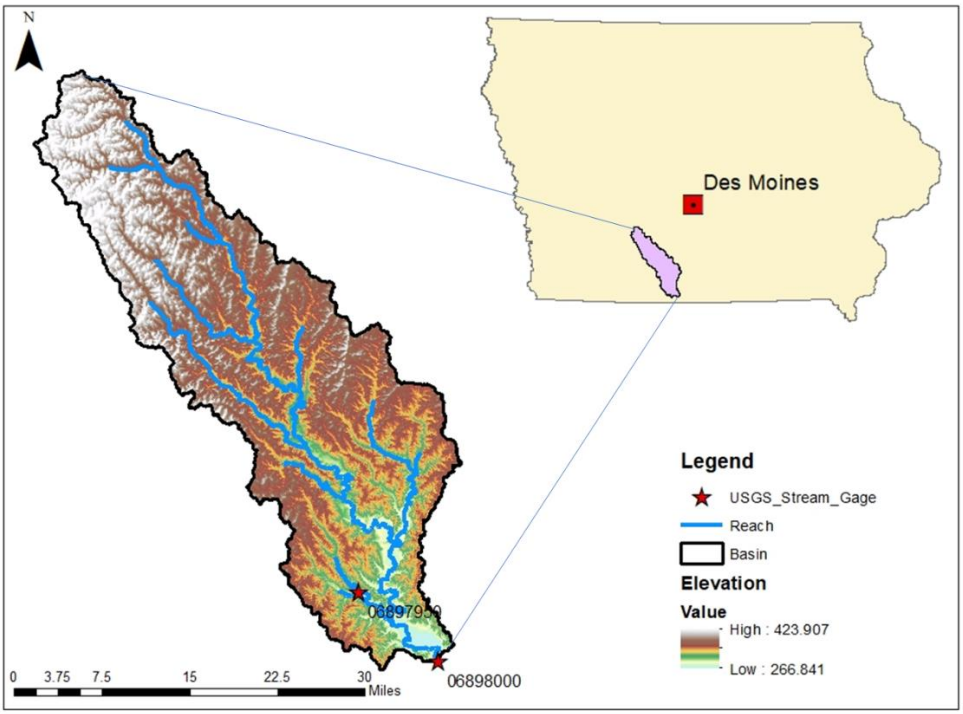

Figure 3.5 Location of North Thompson River basin, IA

The study area shows the land use distribution of 45% pasture/grassland, 41% cropland, which is distributed more in the upper basin, and 4% deciduous forest land.

The upper portion of the study area is dominated by silty clay loam with soil series of Sharpsburg and taxonomic class of fine, smectic, mesic Typic Argiudolls, and the lower part is dominated by clay loam soil with Shelby soil series and taxonomic class of fine-loamy, mixed, super active, mesic Typic Argiudolls.

3.1.1.5 Upper Big Sioux River Watershed, SD (UBR)

The Big Sioux River begins near the town of Summit, South Dakota. The watershed consists of the geological formation of Coteau des Prairies, a flatiron-shaped rolling plateau. The Big Sioux River Basin includes Upper Big Sioux, Middle Big Sioux, and Lower Big Sioux. The study area, Upper Big Sioux River Watershed (HUC 1010170201), lies lower small part of Marshall, part of Day, part of Roberts, part of Grant, part of Clark, part of Hamlin, part of Deuel, and a major part of Codington counties, SD. The watershed has an area of 3931sq km (Figure 3.6) The study area is dominated by soil series of Forman and taxonomic class of fine-loamy, mixed, superactive, frigid Calcic Argiudolls.

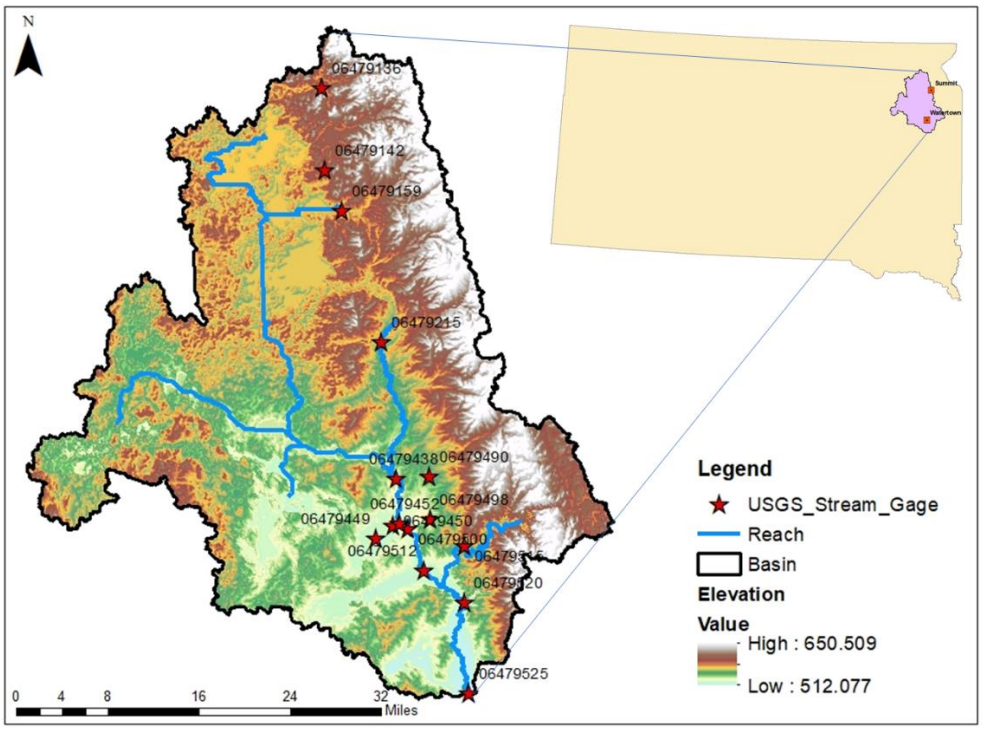

Figure 3.6 Location of Upper Big Sioux River Watershed, SD

3.1.2 Data Acquisition and Model setup

The software ArcMap 10.5.1 (Maguire, 2008) and ArcSWAT 2012 (Arnold et al., 2012a) were used to model the watersheds. The input data were collected from various sources.

The elevation data (DEM) (10-m resolution) and National Hydrography Data were obtained from the United States Geological Survey (USGS) National Map Viewer (U.S. Geological Survey, 2019a). The land cover data was obtained from Multi-Resolution Land Characteristics (MRLC) Consortium—National Land Cover Data (NLCD) available at a 30-m resolution for the U.S (U.S. Geological Survey, 2019b) . The land cover categories include cropland, developed area, pasture, range, forest,

wetland, barren, and water. The observation data of streamflow were downloaded for each watershed from USGS measuring gage station. The soil data from Soil Survey Geographic Database (SSURGO) were downloaded from the USDA Web Soil Survey (Soil Survey Staff, 2021). Required weather data including sub-daily rainfall and daily maximum and minimum temperature data were obtained from NOAA Climate Data Online (NOAA National Centers for Environmental Information (NCEI), 2005) for all watersheds except Cypress Creek and Headwaters Labette Creek. Sub-daily rainfall data for Cypress Creek and Headwaters Labette Creek were obtained from Harris County Flood district (Harris County Flood Warning System, 2020) and Mesonet KS State, respectively (Weather data Library Kansas Mesonet, 2020).

3.1.2.1 Manipulation of GIS Data

More than one raster files of DEM, NLCD, and soil were merged using ‘Mosaic To New Raster’ tool. The merge raster datasets were clipped for the domain using ‘clip raster tool’ in ArcMap. This tool allows to extract a portion of raster data based on the provided extent. Then the clipped raster dataset was projected to NAD_1983_UTM_Zone_14N coordinate system. The prepared raster datasets were input in the SWAT interface. The NLCD and soil data were then reclassified according to the SWAT defined classification.

3.1.2.2 Model Setup and Parameterization

The model was set up in the ArcSWAT interface. The watersheds were first

delineated, and flow accumulation and subbasins were created from elevation raster data (DEM/LiDAR). Flow accumulation was later matched to channels, and a channel was defined for each subbasin. Loadings (mass of pollutants, e.g., pounds of sediments or nitrate) from the subbasin enter the channel network of the watershed in the associated reach segment. Outflow from the upstream reach segment(s) will also enter the reach segment. Processes involved in routing water in channels are handled in a separate subroutine. Hydrologic response units (HRUs) are portions of a subbasin that possess unique land use/management/soil attributes (Arnold et al., 2012a). Hydraulic response units (HRU) were defined within the watershed using landuse data, soil, and two classes of the slope with threshold values of 10%, 10%, and 15% for land use, soil, and slope, respectively. Observed sub-daily precipitation and average daily temperature data were used and a world weather database was installed to help generate time series of relative humidity, solar radiation, and wind speed. With the use of a base flow filter, the base flow was determined for the observed discharge and substrate from the discharge data for few observed data sets. The model was run with the GAML method. For the GAML option, the rainfall-runoff method was selected as the Sub-daily Rain/G&A/Hourly route option. Based on data availability, model calibration and validation periods were defined (Table 3.2). The model outputs were obtained on daily basis.

Table 3.2 Time windows for model calibration and validation

Watershed	Warmup years	Calibration	Validation
Cypress Creek (CYC)	2007 - 2008	2009 – 2013	2014 – 2017
Clear Creek (CLC)	2009	2010	2017
Headwaters Labette Creek (HWC)	2012	2013	2014
North Thompson River Basin (NTR)	2010	2011	2012
Upper Big Sioux River (UBR)	2009	2010-2011	2013

3.1.3 Model Calibration and Validation

Warmup period is essential for the short-term simulation to get the hydrological cycle fully operational during the real simulation period. Model calibration was carried out by adjusting the selected parameters in the model to obtain the best fit between the simulated flow and the observed flow data. Initially, the model was executed without any parameter adjustments. The results at this stage were then analyzed to check the quality of default parameters with respect to calibration target values. Through the literature review process, ten parameters were selected to adjust in this study: saturated hydraulic conductivity (SOL_K), initial SCS runoff curve number for moisture condition II (CN2), an available water capacity of the soil layer (SOL_AWC), Manning's "n" value for overland flow (OV_N), threshold depth of water in the shallow aquifer required for

return flow to occur (GWQMN), groundwater "revap" coefficient (GW_REVAP), average slope steepness (HRU_SLP), effective hydraulic conductivity in tributary channel alluvium (CH_K(1)), Manning's "n" value for the main channel (CH_N(2)), and maximum canopy storage (CANMAX) (Arnold et al., 2012b). A sensitivity analysis was done, and the most sensitive parameters were identified (Feyereisen et al., 2007). The calibration process is most effective when the highly sensitive parameters are the first to be adjusted. Sensitivity can be measured by changing an input parameter, then calculating the resultant change of the output. A local sensitivity analysis changes one parameter at a time, and this method was used for the project. The equation (1) for sensitivity index, shown below, is a method used to determine the sensitivity of each parameter.

$$Si = \frac{Xd}{Yd} * \frac{Ymax - Ymin}{Xmax - Xmin} \qquad (3)$$

To find the sensitivity of each parameter, three simulations must be performed. First, the default simulation is completed, with X_d representing the model's default parameter value and Y_d representing the average value of the outputs. Next, the acceptable maximum and minimum values for each input parameter are defined and represented as X_{max} and X_{min} (respectfully). These values were determined via literature review (Jha, 2011). Then, two more simulations can be performed, one each using X_{max} and another using X_{min}. The respective average output values are represented by Y_{max} and Y_{min}. Once these values are inserted in the sensitivity index equation, a normalized value is determined, allowing easy comparison between multiple parameters. After the sensitivity index of each parameter has been calculated, the parameters are

ranked in order of sensitivity, and calibration is performed in this sequence.

The calibration process was carried out with manual calibration using ArcSWAT's Manual Calibration Helper. The daily model outputs of each watershed were compared with the average daily discharge data at the appropriate USGS measuring gauges, which are located at the closing point of each watershed outlet.

The model performance was examined using visualization of figures and then further evaluated and rated by three statistical measures: the Nash-Sutcliffe efficiency (NSE), Root Mean Squared Error (RMSE) – observations standard deviation ratio (RSR), and Percent Bias (PBIAS) (Moriasi et al., 2007) (Table 3. 3). After successful calibration with acceptable statistical measures, the validation process was carried out. The same statistical measures were used to evaluate the validation process.

Table 3. 3 Summary of the ratings of goodness of fit. Reprinted from [Model Evaluation Guidelines for Systematic Quantification of Accuracy in Watershed Simulations by Moriasi et al., 2007]

Rating	RSR	NSE	PBIAS
Very Good	$0.00 \leq RSR \leq 0.50$	$0.75 < NSE \leq 1.00$	$PBIAS < \pm 10$
Good	$0.50 < RSR \leq 0.60$	$0.65 < NSE \leq 0.75$	$\pm 10 \leq PBIAS < \pm 15$
Satisfactory	$0.60 < RSR \leq 0.70$	$0.50 < NSE \leq 0.65$	$\pm 15 \leq PBIAS < \pm 25$
Unsatisfactory	$RSR > 0.70$	$NSE \leq 0.50$	$PBIAS \geq \pm 25$

3.2 Comparing the calibrated soil parameters with estimated soil parameters

3.2.1 Estimation of soil parameters

The pedotransfer functions (PTF) developed by Rawls (Rawls et al., 1998) were used to estimate saturated hydraulic conductivity (SOL_K) and soil available water content (SOL_AWC). The equations were derived according to USDA soil textural classes and two bulk density classes. The PTF by Alexander (1980) was used to estimate bulk density (SOL_BD) in this study.

3.2.1.1 Saturated Hydraulic Conductivity (SOL_K)

Rawls et al. (1998) modified Ahuja's saturated hydraulic conductivity – effective porosity relationship as the exponent component was redefined as 3 minus the Brooks-Corey pore size distribution index (λ) (Ahuja et al., 1985), (Rawls et al., 1998). Brooks-Corey pore size distribution index was derived from readily available soil water properties (Brooks and Corey, 1964; Rawls et al., 1982). In this study, the following equation (2) was used to estimate SOL_K:

$$\text{SOL\_K} = 1930\ (\phi)^{(3-\lambda)} \quad (4)$$

where, ϕ is effective porosity in m^3/m^3 and λ is Brooks Corey pore size distribution index. ϕ is calculated by following equation:

$$\Phi = (\theta_s - \theta_{33}) \quad (5)$$

where θ_s and θ_{33} is soil moisture at 0 kPa (saturated soil moisture) and -33 kPa,

respectively. θ_s and θ_{33} are estimated using equations 4 and 5 (Saxton and Rawls, 2006).

$$\theta_s = \theta_{33} + \theta_{(s-33)} - 0.097SA + 0.043 \quad (6)$$

$$\theta_{33} = \theta_{33t} + (1.283(\theta_{33t})^2 - 0.374\theta_{33t} - 0.015) \quad (7)$$

$$\theta_{33t} = 0.251SA + 0.195CL + 0.011OM + 0.006(SA * OM) - 0.027(CL * OM) + 0.452(SA * CL) + 0.299 \quad (8)$$

$$\theta_{s-33} = \theta_{(s-33)t} + (0.6360_{(s-33)t} - 0.107) \quad (9)$$

$$\theta_{(s-33)t} = 0.278S + 0.034CL + 0.022OM - 0.018(SA * OM) - 0.027(CL * OM) - 0.584(SA * CL) + 0.078 \quad (10)$$

where, θ_{33t} and $\theta_{(s-33)t}$ are first solution of soil moisture at -33 kPa and (0kPa – 33kP), respectively. SA, CL, OM are sand, clay, and organic matter percent of soil at weight basis, respectively.

Brooks Corey pore size distribution index (λ) is estimated by equation 8.

$$\lambda = \frac{[\ln(\theta_{33}) - \ln(\theta_{1500})]}{[\ln(1500) - \ln(33)]} \quad (11)$$

where, θ_{1500} is soil moisture at -1500 kPa and estimated as follow:

$$\theta_{1500} = \theta_{1500t} + (0.14 * \theta_{1500t} - 0.02) \quad (12)$$

$$\theta_{1500t} = -0.024SA + 0.487CL + 0.006OM + 0.005(SA * OM) - 0.013(CL * OM) + 0.068(SA * CL) + 0.031 \quad (13)$$

3.2.1.2 Soil available water content (SOL_AWC)

Saxton and Rawls (2006) developed regression equations for soil moisture at the tension of -1500 kPa, -33 kPa, and 0 kPa correlated with sand, clay, and organic matter

content. In this study, SOL_AWC is estimated as the difference between θ_{33} and θ_{1500} by the equations 5 and 10, respectively.

3.2.1.3 Soil bulk density (SOL_BD)

Alexander (1980) developed an equation relating the bulk density with the organic carbon content of the soil as the author suggested adding more independent factors did not decrease the standard error significantly, and the proposed equation is not site-specific (Alexander, 1980). The proposed equation (equation 12) was used in this study to estimate SOL_BD.

$$\mathrm{SOL-BD} = 1.72 - 0.294(\mathrm{OC})^{0.5} \quad (14)$$

To estimate the above-mentioned three soil parameters, raw inputs of soil texture (% sand, silt, and clay) and percentage of organic carbon content of each soil type in each watershed were acquired from the NRCS SSURGO database. SWAT reclassified SSURGO soil classes based on the map unit key of soil (MUKEY). SSURGO database from SWAT modeling files was used to gather the information of soil texture and organic matter content for the soil parameter estimation.

3.2.2 Evaluation of model performances

There were two sets of soil parameters derived by two methods: calibrated and calculated (estimated by pedotransfer function). To compare the means of SOL_K between two methods of calculated and calibrated, the independent group t-test was conducted. The ‘ttest’ procedure (‘proc ttest’) was used in SAS 9.4 to check whether the

means of the two groups are significantly different or not at the $\alpha = 0.05$ level.

Models of each watershed were simulated again with calculated soil parameters (SOL_K, SOL_AWC, and SOL_BD). Three statistical measures (NSE, RSR, and PBIAS) were used to evaluate model performances against observed streamflow. Statistical results to were compared to ensemble simulation of regular calibration of all parameters.

3.3 Analyzing the potential deficiency in existing pedotransfer functions applied for native prairie soils

3.3.1 Measurement of soil parameters

Soil hydraulic conductivity was measured in selected watersheds. For this study, two prairie watersheds were selected considering different soil types and land use throughout the watersheds: Cypress Creek watershed (CYC) and Clear Creek watershed (CLC), which are in the tallgrass prairie region in Texas, to measure SOL_K. A total of 26 test sites were selected (15 in CYC and 11 in CLC) (Figure 3.7). The measurement

sites cover land use of native prairie land, ranches, and crop land.

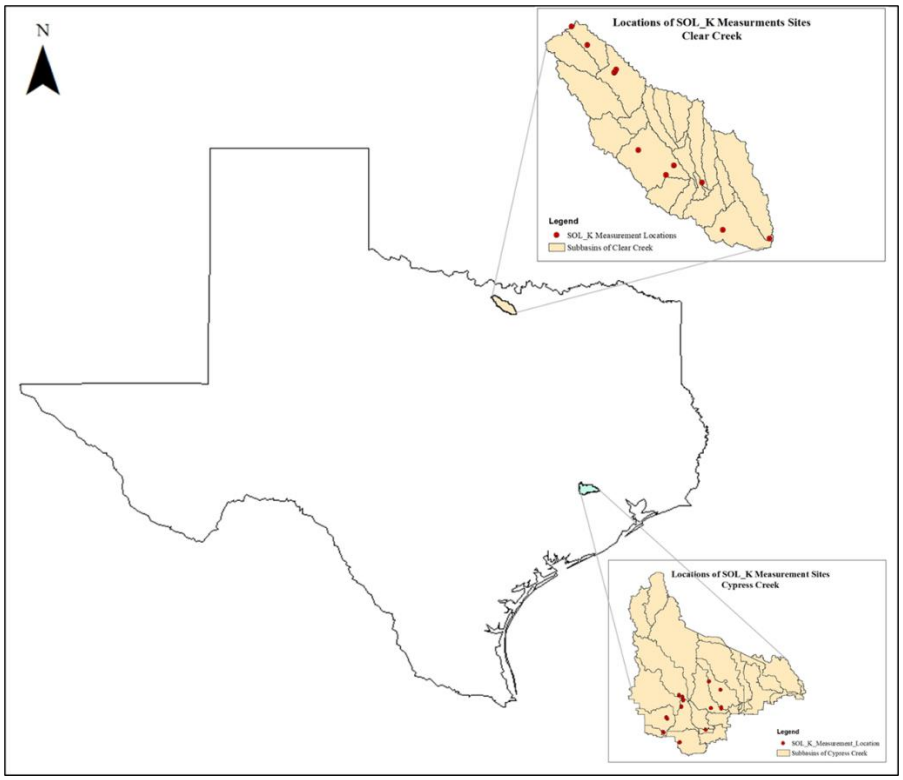

Figure 3.7 Locations of study areas and SOL_K measurement sites: Cypress Creek and Clear Creek

Measured SOL_K (mm/hr) of Cypress Creek were obtained from Harris County Flood District for comparison to field data collected. The SOL_K measurements at mm/hr with two replicates were taken in Cypress Creek using A dual head infiltrometer (Decagon Services, inc., Pullman Washington). A total of 11 test sites were chosen in Clear Creek watershed to do the measurement of SOL_K (mm/hr) (Figure 3.7). At CLC, SOL_K was measured using double ring infiltrometer (double-ring infiltrometer (Turf-Tec International, Tallahassee, Florida) (Figure 3.8). The infiltration rings have a 6-inch inner ring and a 12-inch outer ring with a 7-inch height. Following the American Society

for Testing and Materials (ASTM) D3385, infiltration rate was measured by installing the double ring by driving into the soil. The outer ring prevents the lateral flow and promotes the one-dimensional vertical flow beneath the inner ring. Readings of water level were taken every 15 mins to estimate the SOL_K until get the constant water depth.

Figure 3.8 SOL_K measurement with double ring infiltrometer at Clear Creek watershed

3.3.2 Description of PTFs used

For this study, nine widely used published PTFs were used based on soil texture, effective porosity, and bulk density to estimate the SOL_K (Table 3.4). Cosby et al. (1984) model the SOL_K based on soil textural classes. Ahuja et al. (1989) developed an equation for SOL_K with effective soil porosity based on the generalized Kozeny-Carman equation. Rawls et al. 1998 modified Ahuja's saturated hydraulic conductivity – effective porosity relationship as the exponent component was redefined as three minus

the Brooks-Corey pore size distribution index (λ) (Ahuja et al., 1985; Rawls et al., 1998). Brooks-Corey pore size distribution index was derived from easily available soil water properties such as water content at different pressure heads (Brooks and Corey, 1964; Rawls et al., 1982). Moreover, Timlin et al. (1999) developed PTF based on effective porosity with Brooks-Corey pore size index. Suliman and Ritchie (2001) published a model related to the SOL_K with relative effective porosity defined as effective porosity divided by field capacity (Suleiman and Ritchie, 2001). In 1985, Puckett et al. developed an equation to estimate SOL_K of Ultisols with only one predictor of percentage of clay (Puckett et al., 1985) in lower coastal plains.

Table 3.4 Overview of selected published PTFs used for this study

References	Number of samples	Equation	R^2
(Cosby et al., 1984)	1448	$\text{SOL\_K} = 60.96 * 10^{0.0126*\text{Sand}-0.0064*\text{clay}-0.6}$	0.872
(Puckett et al., 1985)	42	$\text{SOL\_K} = 4.36 * 10^{-5} * e^{-0.1975*\%\text{clay}}$	0.77

(Saxton et al., 1986)	230	$\text{SOL\_K} = 2.778 * 10^{-6}\{\exp[12.012 - 0.0755(\%\text{sand}) + [-3.8950 + 0.03671(\%\text{ sand}) - 0.1103(\%\text{ clay}) + 8.7546 * 10^{-4}(\%\text{ clay})^2](1/\theta s)]\}$	0.95
(Wösten and van Genuchten, 1988)	1139	$\text{SOL\_K} = \exp\left[7.755 + 0.0352 * \text{silt} + 0.93 - 0.967 * \text{BD}^2 - 0.000484 * \text{clay}^2 - 0.000322 * \text{silt}^2 + {}^{0.001}/_{\text{silt}} - {}^{0.0748}/_{\text{OM}} - 0.643 * \ln(\text{silt}) - 0.01398 * \text{BD} * \text{clay} - 0.1673 * \text{BD} * \text{OM} + 0.02986 * \text{clay} - 0.03305 * \text{silt}\right]$	0.94
(Ahuja et al., 1989)	473	$\text{SOL\_K} = 764 * \Phi^{3.288}$	0.670
(Rawls et al., 1998)	900	$\text{SOL\_K} = 1930\Phi^{(3-\lambda)}$	0.92
(Timlin et al., 1999)	N/A	$\text{SOL\_K} = 2.59 * 10^{-4} * 10^{0.6\lambda} * \Phi^{2.54}$	N/A
(Suleiman and Ritchie, 2001)	N/A	$\text{SOL\_K} = 12302 * \Phi^{3.63}$	0.58
(Weynants et al., 2009)	136	$\text{SOL\_K} = \exp(1.9582 + 0.0308 * \text{sand} - 0.6142 * \text{BD} - 0.01566 * \text{OC})$	0.25

3.3.3 Estimation of saturated hydraulic conductivity and evaluation of published PTFs

The selected nine published PTFs were used to estimate SOL_K at the test sites

of study areas with predictors obtained from the NRCS web soil survey. To evaluate the predictive capability of PTFs, we chose two widely used statistical measure: (1) Coefficient of determination (R^2) which assess how strong is the linear relationship between two variables (Equation 15); (2) Root means square error (RMSE) of prediction which gives the standard deviation of prediction residuals (Equation 16) (Chicco et al., 2021).

$$R^2 = 1 - \frac{\sum_{i=1}^{m}(Xi-Yi)^2}{\sum_{i=1}^{m}(\bar{Y}-Yi)^2} \quad (15)$$

$$RMSE = \sqrt{\frac{1}{m}\sum_{i=1}^{m}(Xi - Yi)^2} \quad (16)$$

Where Yi is the measured SOL_K, Xi predicted value of SOL_K at *i* location, m number of measurements. For the best predictive capability, the RMSE should be low as possible and R^2 should approaching 1.

3.4 Development and evaluation of a new pedotransfer function

3.4.1 Description of study areas

Two watersheds were chosen in Texas for this study. The first is Cypress Creek Watershed (CYC), located in the Western Gulf Coastal plain in Texas. It lies in Harris County and Waller County. The dominant soil in the study area is sandy clay loam. The second is the Clear Creek Watershed (CLC) of the Trinity River watershed lies in Denton, Wise, Cooke, and Montague counties, Texas. The dominant soil of this watershed is gravelly clay loam and clay.

The drainage area of Cypress Creek and Clear Creek were 552 sq. km and 766

sq. km, respectively. Both watersheds have the dominant land use of hay/pasture, covering more than 90% of the total area.

3.4.2 Soil and Vegetation data

Soil Survey Geographic Database (SSURGO), the compilation of soils information collected by the Natural Resources Conservation Service (NRCS) were used to conduct the study. Cypress Creek has 11 soil series, and Clear Creek has 20 soil series. Soil information of soil texture (%) (Figure 3.9), and organic carbon content (%) for each series was obtained from SSURGO database for the regression analysis. Vegetation information in each watershed was acquired from the Texas parks and wildlife website (tpwd.texas.gov) (Figure 3.10).

The vegetation was identified in the test sites based on the observation and the vegetation map (Table 3.5 and Table 3.6). The dominant species were considered for regression analysis. In the study areas, the dominant species found at prairie land are Bermuda grass and Little blue stem. The crop land consists of major crops of corn and soybean. The oak tree is the most common woody vegetation, found in the study area.

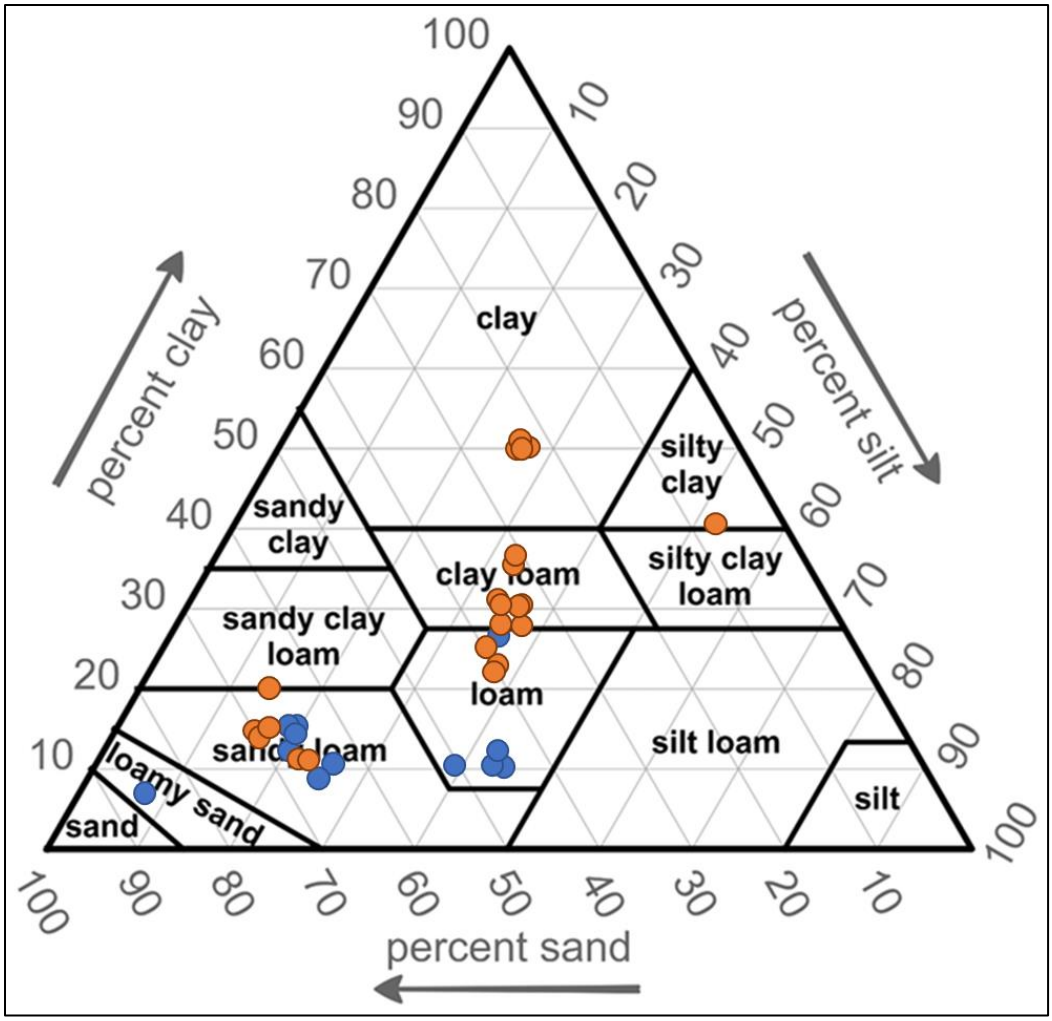

Figure 3.9 Textures of soil series found in study areas (blue dots for Cypress Creek and orange dots for Clear Creek). The texture triangle is based on USDA soil texture classification

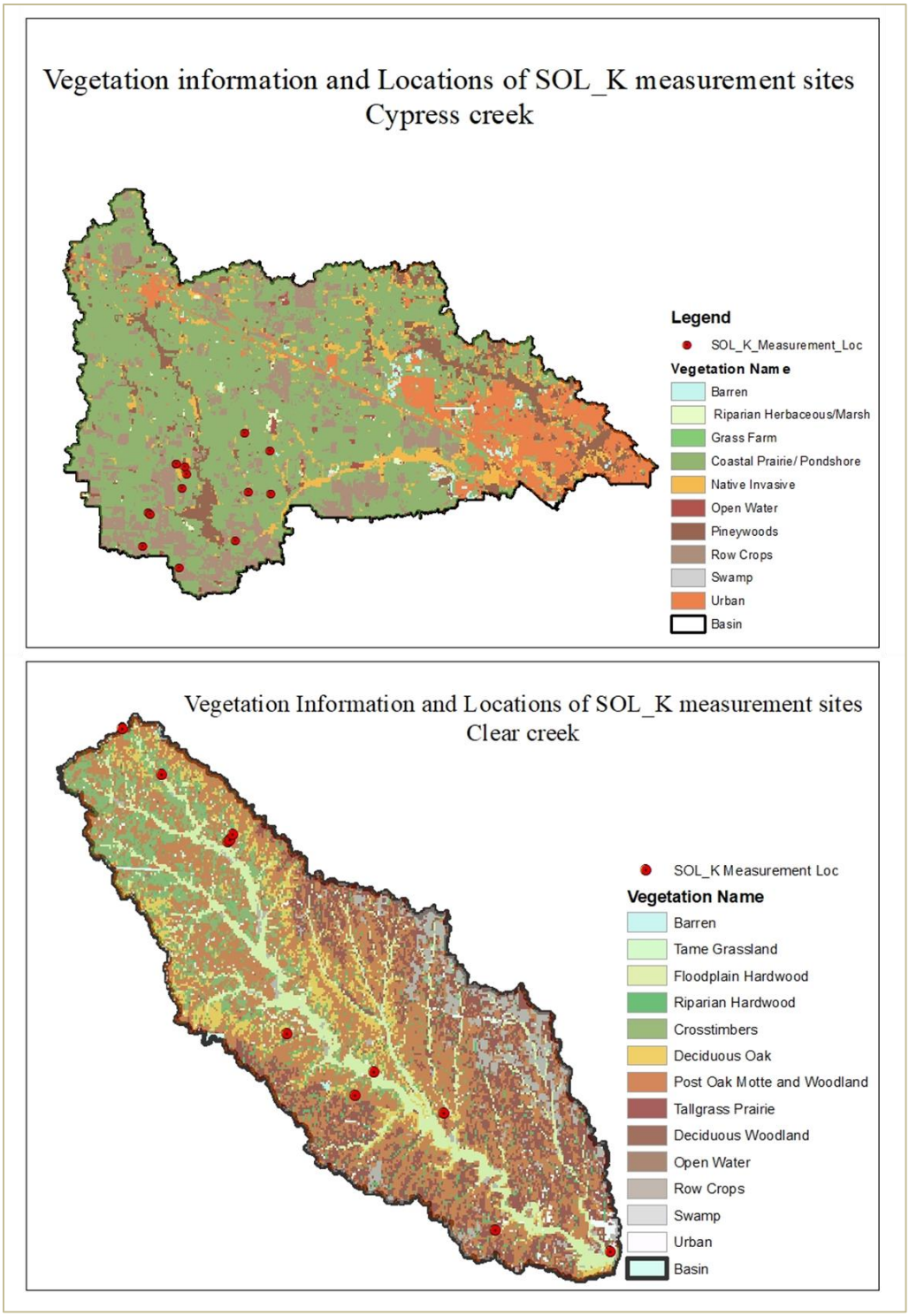

Figure 3.10 Vegetation information and locations of SOL_K measurement sites of study area

Table 3.5 Information of soil, vegetation, and land-use of test sites at Cypress Creek watershed

Site name	Soil Name	Land use	Dominant vegetation
Upper Tucker Prairie	Wockley	Prairie	Bermuda grass, King ranch bluestem, Little bluestem
Lower Tucker Prairie	Monaville	Prairie	Bermuda grass, King ranch bluestem, Little bluestem
Warren Prairie	Gessner	Prairie	Bermuda grass, King ranch bluestem, Little bluestem
Warren Wet Prairie	Gessner	Wet Prairie	Corn, Soybean
Upper Tucker Wet Prairie	Nahatche Loam	Wet Prairie	Water oak, Sweetgum, Sugar hackberry, Southern red oak, River birch, American elm
Nelson Rice	Katy	Rice	Rice
Chase North Rice	Katy	Rice	Rice
Warren Millet	Gessner	Row Crop	Millets: Paspalum
Warren Pasture	Hockley	Pasture	Bermuda grass, King ranch bluestem, Little bluestem
Lower Tucker Pasture	Monaville	Pasture	Bermuda grass, King ranch bluestem, Little bluestem

Bing	Katy	Pasture	Bermuda grass, King ranch bluestem, Little bluestem
Manor	Katy	Pasture	Corn, Soybean

Table 3.6 Information of soil, vegetation, and land-use of test sites at Clear Creek watershed

Site name	Soil Name	Land use	Dominant Vegetation
Dickinson water Foundation1	Gaddy	Grazed Pasture	Bermuda, Switchgrass
Dickinson water Foundation2	Sanger	Native prairie land	King Ranch Bluestem, Bermuda
Scott's private land1	Windthorst	Ploughed land	Pecan, Post oak, White ash, Green ash, American elm, Sugar hackberry
Scott's private land2	Bolar	Rotating grazing	Little blue stem, Silver bluestem, Texas Winter grass, Sideoats grama, Bermuda
Sanger sports park	Frio	Grass land	Bermuda grass/Oak
Sanger Ranch	Medlin	Ranch	Little bluestem, King ranch Bluestem
Pasture1	Hensley	Pasture	Bermuda, King ranch

			Bluestem
Pasture2	Bolar	Pasture with rag weed	King ranch bluestem, Bermuda, Ragweed
Don Vogel Ranch1	Bosque	Pasture - Coastal Bermuda grass	Bermuda Grass
Don Vogel Ranch2	Bosque	Pasture/Oak	Post oak, American elm
Don Vogel Ranch3	Venus	Prairie land - Canada wild Rye	Bermuda, Canada wildrye

3.4.3 Specific root length (SRL)

In our study, the SRLs of selected species were obtained from various research papers, and a few were calculated using the following two equations.

$$SRL = {}^{L}/_{m} \quad (17)$$ (Ostonen et al., 2007)

$$SRL = {}^{4}/_{(RTD * D^2 * \pi)} \quad (18)$$ (Ostonen et al., 2007)

where SRL is specific root length in m/g, L is root length in m, m is dry mass of root in g, RTD is root tissue density in g/m3, and D is the diameter of root in m. The information of root length and dry mass of root were obtained from previous studies to calculate SRL. Table 3.7 showed the SRL of selected plant species used in our study.

Table 3.7 Specific root length values of plants species

Species	Common name	SRL, m/g	Source
Cynodon dactylon	**Bermuda grass**	43.14	(Bo and David, 2019; Fuentealba et al., 2015)
Bouteloua gracilis	**Blue grama**	102.71	(Craine et al., 2003)
Poa pratensis	**Kentucky bluegrass**	207.06	(Craine et al., 2003)
Schizachyrium scoparium	**Little bluestem**	102.69	(Craine et al., 2003; Rebecca Nelson et al., 2010)
Sorghastrum nutans	**Indian grass**	59.29	(Rebecca Nelson et al., 2010)
Andropogon gerardi	**Big bluestem**	61.00	(Craine et al., 2003; Rebecca Nelson et al., 2010)
Panicum virgatum	**Switch grass**	19.69	(Rebecca Nelson et al., 2010)
Zea mays	**Corn**	28.81	(Chen et al., 2014; Fernández et al., 2009; Lyu et al., 2016; Souza et al., 2016)
Glycine max	**Soybean**	51	(Fernández et al., 2009)
Oryza sativa	**Rice**	750	(Gu et al., 2017; Li et al., 2017; Zhang et al., 2019)
Paspalum L.	**Paspalum**	37.5	(Bo and David, 2019)

Setaria italica	**Foxtail millet**	466.52	(Ahmad et al., 2018)
Pinus massoniana	**Pine tree**	8	(Yang et al., 2021)
***Betula lenta* L.**	**Sweet birch**	100	(Comas et al., 2014)
***Quercus rubra* L.**	**Red oak**	62.5	(Comas et al., 2014)
Ulmus rubra	**Slippery elm**	80	(Comas et al., 2014)
Nyssa sylvatica	**Black gum**	58	(Comas et al., 2014)

3.4.4 Regression Analysis and development of new pedotransfer function

Pearson correlation analysis was carried out to analyze the correlation patterns among SOL_K and soil texture, organic carbon, and SRL. Correlation analysis was done using SAS 9.4 (SAS Institute, Cary, North Carolina) with the correlation procedure ("Proc corr").

Based on the correlation patterns, a new relationship between SOL_K and soil properties was developed using multiple linear regression with SAS 9.4. In this procedure, the 'stepwise' selection option was selected, which results in a combination of forward and backward regression. Here independent variables of the percentage of organic carbon (OC), sand (SA), and silt (SI), and specific root length (SRL), and the interaction effect between variables were added one by one and its significance was tested. Then variables can be added or deleted until the model gets the best fit based on the coefficient of determination (R^2). Stepwise analysis was selected for this study since there was collinearity among soil texture, organic matter, and SRL resulted in presence of one variable might have significant while the presence of another variable.

The last step of the stepwise analysis gave the best estimate of parameters for the regression equation. In this study, stepwise regression proved SD and SRL are the only variables that were the appropriate predictors to estimate SOL_K with limited data. However, based on the literature, soil texture in addition to percentage of sand, and OC should be predictors for SOL_K (Rawls et al., 1998; Rawls et al., 2004). Thus, SI and OC were made compulsory and resulted in a good fit.

3.4.5 Evaluation and validation of the pedotransfer function

The coefficient of determination (R^2) is the standard statistic to evaluate the regression equation (Chicco et al., 2021). R^2 quantifies how much of the dependent variable is estimated from the independent variable in terms of proportional variation. Higher R^2 indicates the better model fit. R^2 and root mean squared error (RMSE) were used to evaluate newly developed PTF (Zhang and Schaap, 2019). Equation 13 and equation 14 are used to calculate the statistics.

These two statistical criteria have no threshold to determine whether the model is good, however we evaluated the model based on the own threshold.

The developed PTF model was validated using a statistical comparison between measured and predicted SOL_K values. For the validation, observed SOL_K at the CLC watershed were used. The same statistical criteria were used to validate the model. In addition to that, a two-sample t-test using SAS 9.4 was done. The model can be validated by applying the PTF model in the hydrological model, and the predicted flow will be evaluated.

3.5 Evaluating the impact of newly developed pedotransfer function on the calibration of SWAT model

3.5.1 Description of Study Areas

We selected four watersheds that have dominant land use of grasslands and croplands across the tallgrass prairie region of the Great Plains in the USA (Table 3.8) for this study. The watershed characteristics were already discussed in section 3.1.1. The tallgrass prairies contain more than 500 prairie species, where four species are dominated among them: big bluestem (Andropogon gerardii), switchgrass (Panicum virgatum), indiangrass (Sorghastrum nutans), and little bluestem (Schizachyrium scoparium) (Grace et al., 2000). Based on the NRCS glossary, grassland can be divided into three categories: hay land, pastureland, and ranch. The hay and pastureland are managed to grow forage crops to be harvested or/and allow for grazing. Ranches have native prairie species. The cropland in this region has row crops, mainly corn, soybean, and wheat. The soil groups in this region are strongly correlated with grass cover and the precipitation pattern. It has a diversity of soil, including Mollisols, Alfisols, Aridisols, Inceptisols, and Entisols (Hirmas and Mandel, 2017).

Table 3.8 Description and vegetation information of study areas

Watershed	Drainage Area (sq. km)	Vegetation

Clear Creek watershed, TX (CLC)	766	Coastal Bermuda, Big bluestem, king ranch bluestem, little bluestem, Switch grass
Headwaters Labette creek watershed, KS (HWC)	554	Big bluestem
North Thompson River basin watershed, IA (NTR)	1799	Big bluestem, Butterfly milkweed, Prairie cord grass, Pale purple coneflower, Pasture - Kentucky bluegrass, bromegrass
Upper Big Sioux River watershed, SD (UBR)	3931	Buffalo grass, Big bluestem, Blue grama grass, Little bluestem, Prairie dropseed, Sideoats grama

3.5.2 Application of the newly developed pedotransfer function (PTF)

The new PTF requires the inputs of soil texture (sand and silt content), soil organic carbon (OC), and specific root length (SRL).

The soil texture and OC were obtained from the SWAT input file, and SRL was added for each HRU based on the land use and the appropriate plant community. SRL values were obtained from previous studies (Bo and David, 2019; Comas et al., 2014; Craine et al., 2003; Fuentealba et al., 2015; Rebecca Nelson et al., 2010). If the HRU had more than one dominant species, then the average SRL or the SRL of dominant species were considered. SOL_Ks of each soil layer for each HRU was estimated using the newly developed PTF. The soil input file (.sol) was then altered with new SOL_Ks and inputted into the model. We ran the model and evaluated the model performances.

The statistical analysis was performed to check the heterogenous SOL_K obtained from each method using SAS with the univariate procedure. The univariate procedure provides the measures of central tendency (mean and median), measures of dispersion (standard deviation), and allow to visualize the SOL_K data by box plot. In this way, the dispersion pattern of SOL_K from each method (calculated, calibrated, and new SOL_K) could be analyzed.

3.5.3 Evaluation of model performance

The two model performances (simulation with regular calibration, simulation with integration of new PTF) were evaluated separately using three statistical measures includes the Nash-Sutcliffe efficiency (NSE), Root Mean Squared Error (RMSE) – observations standard deviation ratio (RSR), and Percent Bias (PBIAS) (Moriasi et al., 2007) and statistically compared the performances.

CHAPTER IV

RESULTS AND DISCUSSION

4.1 Model calibration and validation results

The calibration process was done to minimize the variations among simulated and observed data. The simulated daily streamflow hydrographs of all five watersheds were compared with observed streamflow data at respective watershed outlets. According to the statistical measures for model calibration, defined by Moriasi et al., 2007, overall SWAT simulation matched well with the observed flow (Figure 4.1 and Table 4.1). Among five watersheds, the SWAT model of CYC watershed performed very well based on the Moriasi et al., 2007 rating. As the other four prairieland watersheds are not well covered by a dense network of weather observatory stations with sub-daily rainfall data, which is the primary input, SWAT models of the other four watersheds performed reasonably in terms of NSE, RSR, and PBIAS (the relationship between observatory and predicted flow). Additionally, observed streamflow data from the USGS gauge station are not available for as continuous data.

Initially, models of CYC, CLC, HWC, and UBR over-predicted both peak flows and base flows of streamflow compared to the observed flow. The most sensitive parameter (SOL_K) of the CYC model was reduced to increase the soil permeability and reduce the runoff. Also, the initial SCS runoff curve number for moisture condition II (CN2) was increased to increase the runoff. In SWAT, the infiltration potential of rainfall is influenced by the daily fluctuations of soil moisture content (SMC) via adjusted CN parameter. This is called the daily curve number, or cnday. The cnday parameter goes up

after a rainy day and reduces if dry days continue. The GAML method uses effective hydraulic conductivity (Keff) to adjust potential infiltration heads to reflect SMC. Keff was calculated based on cnday. If cnday is high, Keff tends to be low and vice versa. Since the model overpredicted the base flow, the threshold depth of water in the shallow aquifer, required for the return flow, was increased to reduce the base flow. The peak flows early shifted for some storms. To correct the early shift, the slope (HRU_SLP) was decreased and Manning's n value (OV_N) was increased. The fitted values for all parameters were obtained by adjusting the values within the range until a good match was found between the simulated and observed values.

Initial simulation for NTR seemed under-predicted and missed some of the peaks. As discussed above, SOL_K and CN2 were adjusted inversely (Figure 4.1 d).

The model performances were evaluated using two statistical measures, NSE and RSR. The goodness-of-fit acceptability values are listed in Table 3. 3. The statistical values of NSE and RSR were rated at least 'satisfactory' based on the guidance (Moriasi et al., 2007). Even with reasonable NSE and RSR values, PBIAS resulted in high positive or negative values in some cases. Bias indicates the average tendency of simulated values to be larger or smaller than their observed values. In some instances, SWAT captures the time response of flow well; however, it fails to capture the total volume of flow. This lack-of-fit in total volume is that the rainfall data did not represent the entire watershed well.

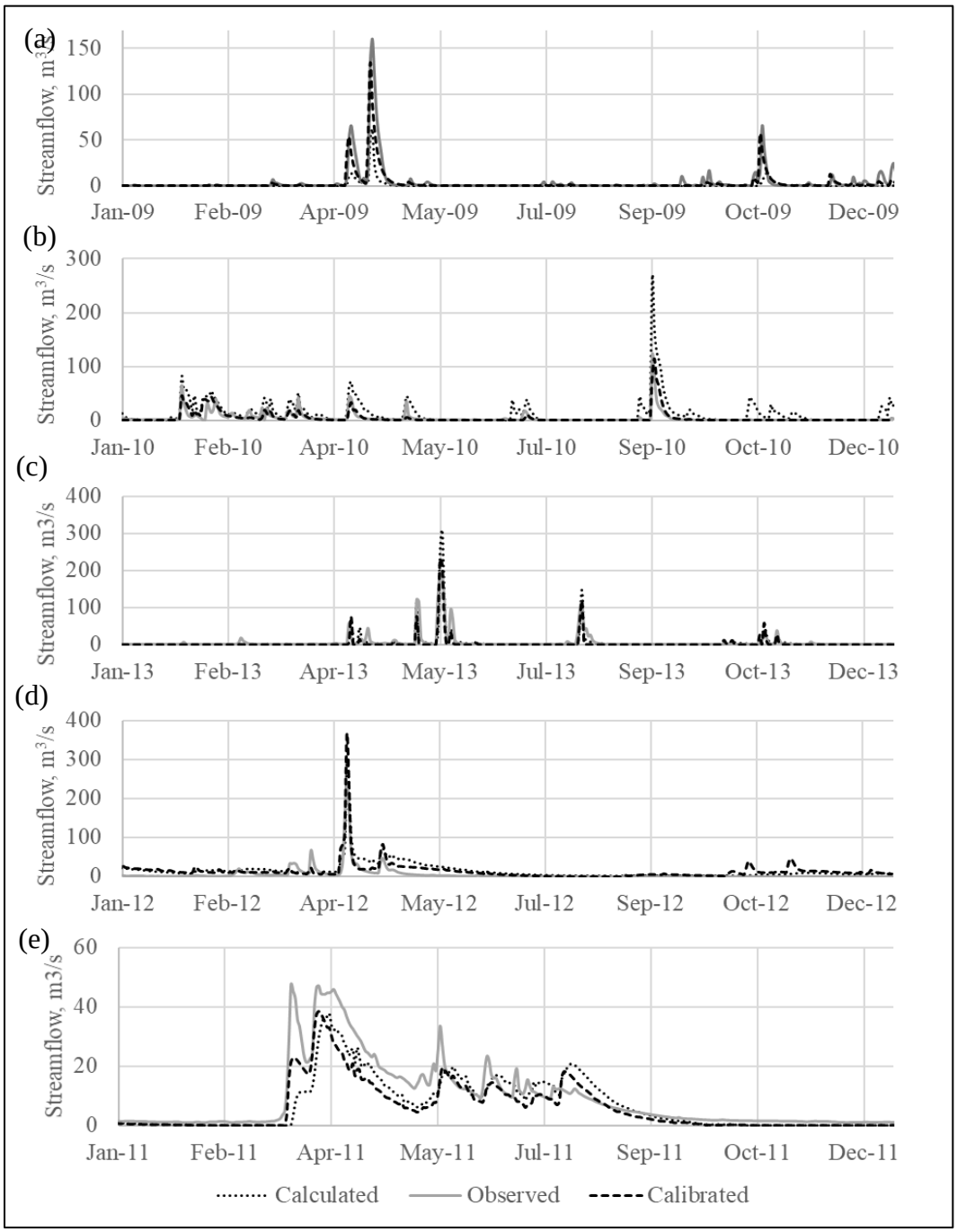

Figure 4.1 Comparison of simulated streamflow by calculated and calibrated soil parameters of (a) Cypress creek watershed, (b) Clear creek watershed, (c) Headwaters Labette creek watershed, (d) North Thompson River basin, and (e) Upper Big Sioux River basin

Table 4.1 Model performance results with rating according to Moriasi et al., 2007

Watershed	NSE		RSR		PBIAS	
	Calibrated	Calculated	Calibrated	Calculated	Calibrated	Calculated
CYC	0.81	0.74	0.43	0.51	45.26	-3.01
	V Good	Good	V Good	Good	Unsat	V Good
CLC	0.63	-1.63	0.61	1.62	-0.37	-201.50
	Sat	Unsat	Sat	Unsat	V Good	Unsat
HWC	0.65	0.30	0.59	0.83	43.19	42.14
	Sat	Unsat	Good	Unsat	Unsat	Unsat
NTR	0.54	0.44	0.67	0.74	15.68	-24.56
	Sat	Unsat	Sat	Unsat	Sat	Sat
UBR	0.63	0.44	0.60	0.74	15.08	-24.56
	Good	Unsat	Sat	Unsat	Sat	Sat

4.2 Analysis of calibrated and estimated soil parameters

The calculated and calibrated soil parameters were compared and analyzed. The box plots in Figure 4.2 showed the distribution of SOL_K from each method. SOL_K distribution for all watersheds shows that the means of calibrated values is less than calculated values. SOL_K of CYC was relatively uniformly distributed for both the methods with few outliers. The calculated SOL_K in CLC ranged from 0.68 – 75.9 mm/hr. There are outliers with SOL_K of greater than 30 mm/hr for the soil texture of fine sandy loam to loamy fine sand which covers 16% of HRUs. Other than those outliers, generally, the calculated SOL_K's fall between 0.68 mm/hr and 6.5 mm/hr for

the rest of the HRUs. However, the calibrated SOL_K falls between 9 mm/hr and 32 mm/hr with an outlier of 100.8 mm/hr for 8% of total HRUs. All the textural classes of fine sandy loam and loamy fine sand have SOL_K of 100.8 mm/hr. The difference between the means of calculated and calibrated values in all watersheds are statistically significant. In HWC, more than 77% of HRUs consist of 24.3 mm/hr and rest of the HRUs consist of SOL_K ranged between 2.7 – 8.1 mm/hr of calibrated SOL_K. However, calculated SOL_K seems more diverse and lies between 1.62 mm/hr and 4.6 mm/hr with few outliers. This indicated that the calibrated values are more general while calculated values are more specific. In UBR, the calibrated values are more general (3 values: 19.4, 64.8, and 66 mm/hr) and uniformly distributed among HRUs. However, calculated values are in a narrow range from 1.84 to 10.7 mm/hr.

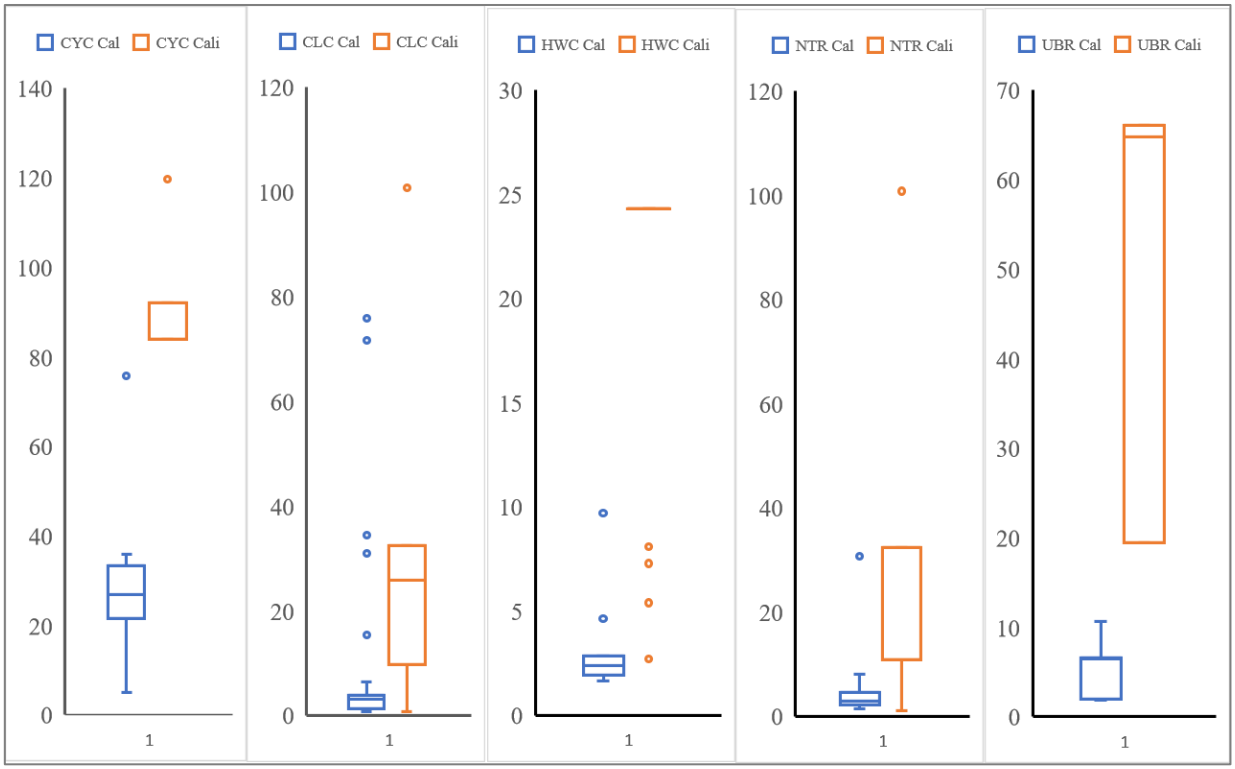

Figure 4.2 Distribution of SOL_K by calculated and calibrated methods for each watershed from left to right (1) Cypress Creek watershed, (2) Clear Creek watershed, (3) Headwaters Labette creek watershed, (4) North Thompson River basin, and (5) Upper Big Sioux River basin

Statistical t-test results indicated the means of SOL_K calculated differ from means of SOL_K calibrated significantly for all the watersheds (Table 4.2). The SOL_K from each method showed quite different was deemed to consider calculated does not reflect the actual physical meaning of the soil.

Table 4.2 The results from statistical t-test

Watershed	Calibrated		Calculated		Pr>F
	Mean	StdDev	Mean	StdDev	

CYC	87.67	6.22	25.93	12.05	<0.0001
CLC	24.57	26.03	8.26	13.77	<0.0001
HWC	20.62	6.92	2.76	1.46	<0.0001
NTR	22.50	20.16	4.45	5.69	<0.0001
UBR	53.08	20.41	4.78	2.46	<0.0001

4.2.1 Comparison of simulations between calculated and calibrated soil parameters

To analyze the soil parameters of native prairie land from existing pedotransfer function, the model performance of calibrated and calculated soil parameters against observed stream flow were compared. Observed steam flow represents the hydrological behavior of watershed both temporally and spatially. The ensemble simulations and the respective model performance results are shown in Figure 4.1 and Table 4.1. The simulation using calibrated soil parameters performed better than the simulation using calculated soil parameters in terms of NSE and RSR.

Figure 4.3 shows the scattered plots of observed versus simulated (from calculated soil parameters and simulated from calibrated soil parameters) stream flows and regression lines for the five watersheds. Flows were separated into the low flow, and high flow and plotted separately for each watershed. A plot of CYC shows both low flow and high flow calibrated simulations tend to behave towards observed flow well compared to calculated. However, in low flow, R^2 (0.23) of calibrated is less than R^2 (0.29) of calculated due to a larger effect of unexplained residuals. Generally low flow R^2 is less than high flow R^2 since low flow had several events and many unexplained

residuals. SWAT model captures the peak flows well and fails to catch the low flows at many events. The total flow did not match with the total observed flow well. This leads to bias between observed and simulated. PBIAS is greater than 25% percent, while NSE and RSR values fall into an acceptable range for all simulations.

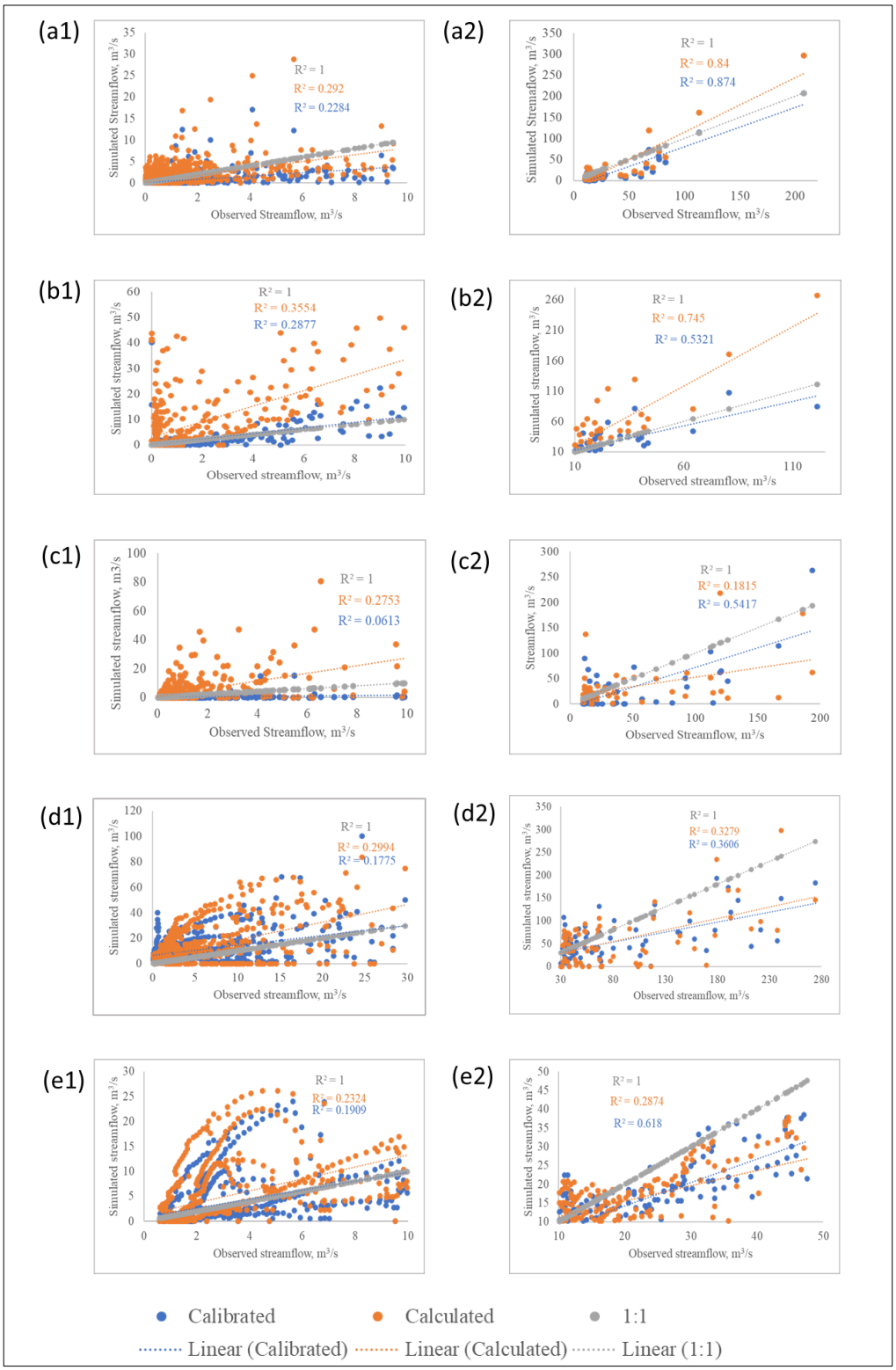

Figure 4.3 Scattered plot of observed stream flow versus simulated stream flow of (a1) CYC low flow, (a2) CYC high flow, (b1) CLC low flow, (b2) CLC high flow, (c1) HWC low flow, (c2) HWC high flow, (d1) NTR low flow, (d2) NTR high flow, (e1) UBR low flow, and (e2) UBR high flow

4.3 Analyzing potential deficiency in existing pedotransfer functions

4.3.1 Input predictors to estimate the SOL_K

Table 4.3 and Table 4.4 show descriptive statistics of input predictors used to estimate SOL_K in Cypress Creek (CYC) and Clear Creek (CLC) watersheds. The predominant soils in the study area of CYC and CLC are fine sandy loam and sandy clay loam, and gravelly clay loam, respectively.

Table 4.3 Descriptive statistics of soil textural information and soil organic matter in Cypress Creek watershed

Statistics	Soil organic matter (OC)	Percentage of clay (CL)	Percentage of silt (SI)	Percentage of sand (SD)
Mean	0.7	11.6	27.2	61.2
Standard Deviation	0.2	4.7	13.0	15.1
Coefficient of variation	29.4	40.1	47.8	24.7
Maximum	1.2	25.0	43.7	85.9
Minimum	0.3	7.5	6.6	38.5

Table 4.4 Descriptive statistics of soil textural information and soil organic matter in Clear Creek watershed

Statistics	Soil organic matter (OC)	Percentage of clay (CL)	Percentage of silt (SI)	Percentage of sand (SD)
Mean	1.0	29.0	33.4	37.6
Standard Deviation	0.4	12.9	9.6	18.2
Coefficient of variation	42.4	44.5	28.9	48.5
Maximum	1.5	50.0	52.0	69.6
Minimum	0.1	11.5	16.4	8.0

4.3.2 The measured SOL_K

The description of test sites and measured SOL_K at CYC and CLC were given in Table 3.5 and Table 3.6 respectively. The measured SOL_K in CYC and CLC ranged from 13 mm/hr to 150 mm/hr and from 16 mm/hr to 156 mm/hr, respectively. Prairie land with dominant species of Bermuda grass is showing more than 30 mm/hr. We observed SOL_K of more than 100 mm/hr in prairie land with dominant species of king ranch bluestem, little bluestem, and big bluestem Croplands with corn, soybean, rice, and millets are having SOL_K ranging between 13 mm/hr and 30 mm/hr. Various studies showed that native prairie soils have high SOL_K compared to cropland, where the soil

is exposed to tillage (ex. SOL_K values of native prairie, restored prairie, no-till corn, and row-crop were 87.66, 22.7, 14.28, and 4.31 mm/hr) (Chandrasoma et al., 2016; Fuentes et al., 2004).

Table 4.5 Description of test sites and measured SOL_K in Cypress Creek watershed

Site	Soil Name	Land use	Measured SOL_K, mm/hr
Upper Tucker Prairie	Wockley	Prairie	126.72±33.89
Lower Tucker Prairie	Monaville	Prairie	120.96±45.22
Warren Prairie	Gessner	Prairie	32.23±1.28
Warren Wet Prairie	Gessner	Wet Prairie	28.75±12.91
Upper Tucker Wet Prairie	Nahatche Loam	Wet Prairie	37.80±26.90
Nelson Rice	Katy	Rice	16.38±12.10
Chase North Rice	Katy	Rice	13.61±8.06
Warren Millet	Gessner	Row Crop	35.99±13.59
Warren Pasture	Hockley	Pasture	85.32±75.82
Lower Tucker Pasture	Monaville	Pasture	151.56±45.22
Bing	Katy	Pasture	14.25±10.38
Manor	Katy	Pasture	19.30±22.56

Table 4.6 Description of test sites and measured SOL_K in Clear Creek watershed

Site	Soil Name	Land use	Measured SOL_K, mm/hr
Dickinson water Foundation1	Gaddy	Grazed Pasture	16.65±18.60
Dickinson water Foundation2	Sanger	Native prairie land	36.00±19.35
Scott's private land1	Windthorst	Ploughed land	57.35±26.37
Scott's private land2	Bolar	Rotating grazing	28.00±4.00
Sanger sports park	Frio	Grass land	21.00±11.00
Sanger Ranch	Medlin	Ranch	60.00±41.04
Pasture1	Hensley	Pasture	48.00±6.00
Pasture2	Bolar	Pasture with rag weed	30.00±10.01
Don Vogel Ranch1	Bosque	Pasture - Coastal Bermuda grass	24.00±4.00
Don Vogel Ranch2	Bosque	Pasture/Oak	32.00±8.00
Don Vogel Ranch3	Venus	Prairie land - Canada wild Rye	48.00±30.51

4.3.3 SOL_K Estimation

Figure 4.4 shows the positive linear relationship of predictive values with measured values to the 1:1 line for CYC. The calculated coefficient of determination (R^2) was indicated in Figure 4.4 and Table 4. 7. Three PTFs (Ahuja et al., 1989, Suleiman et al., 2001, and Wosten et al., 1988) seemed close to the 1:1 line with R^2 of 0.45, 0.44, and 0.66, respectively. The R^2 of two PTFs, Cosby et al., (1984) and Weynants et al., (2009), were relatively high (0.51 and 0.55, respectively), which indicates the effect of outliers and R^2 was not sensitive for that. PTF of Puckette et al., 1985 seemed utterly off from the 1:1 line. It should be noted that the PTF of Puckette et al., (1985) used only one predictor (CL) to estimate SOL_K. The dominant soil in CYC is fine sandy loam. Among 9 PTFs, the PTF of Wosten et al., 1988 predicted the best in CYC.

Although R^2 of a few PTFs shows a good correlation between measured and predicted SOL_K, RMSE values of all the PTFs are high and unacceptable (Table 3.6). RMSE is sensitive to outliers. In terms of RMSE, none of the PTFs predicted SOL_K accurately.

Figure 4.5 shows that none of the PTFs predicted SOL_K well in the CLC watershed in terms of R^2. R^2 showed a lack of correlation between predicted SOL_K and measured SOL_K in CLC (Table 4. 7). However, the PTF of Wosten et al., (1988) behaves slightly better among other PTFs in terms of RMSE. Overall, selected published PTFs failed to predict SOL_K in prairie soils in this study. This indicates that current predictors of soil texture, porosity, and organic matter may be inadequate to reflect the actual SOL_K of native prairie soils.

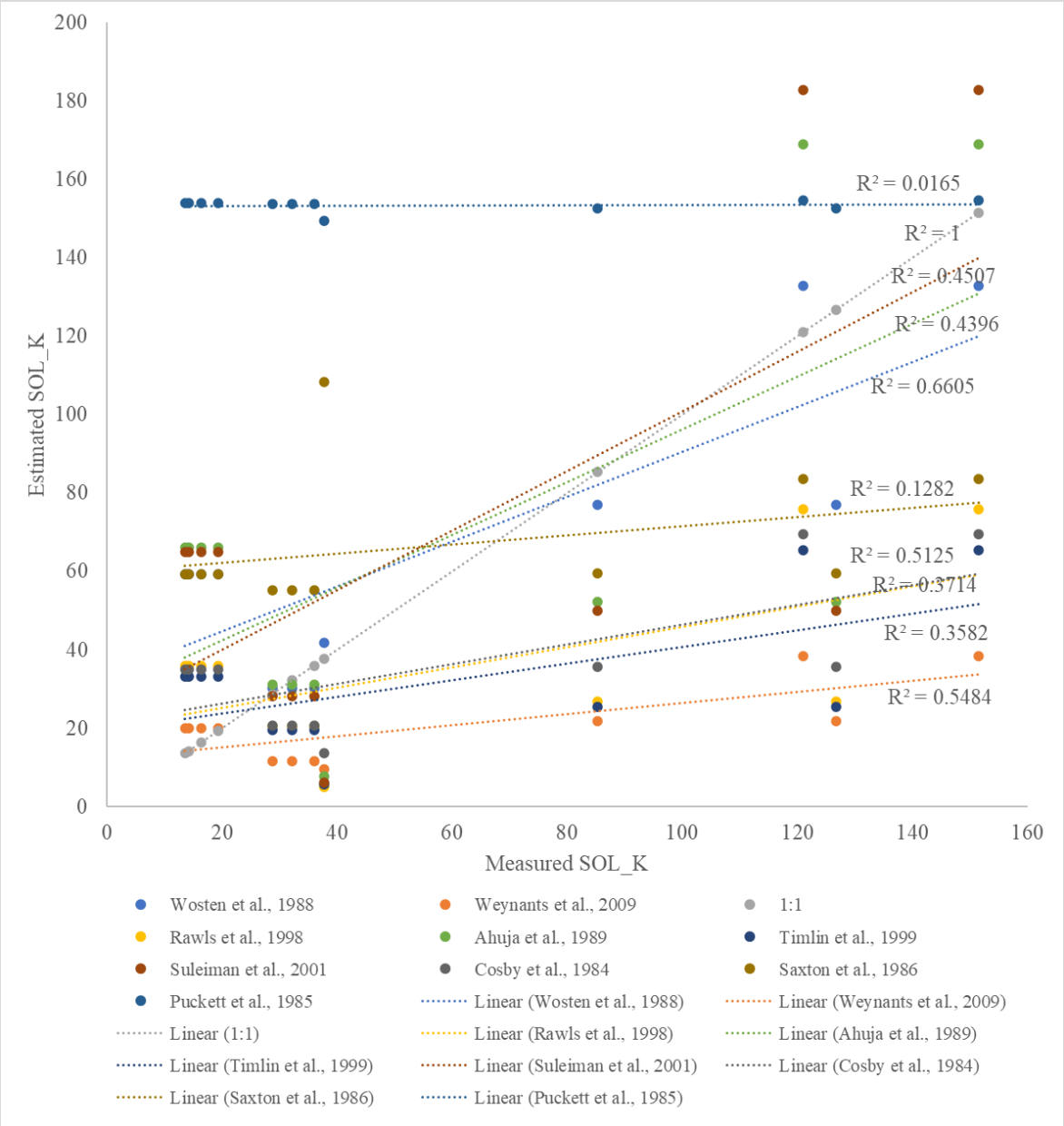

Figure 4.4 Scattered plot of predicted and actual SOL_K in Cypress Creek watershed

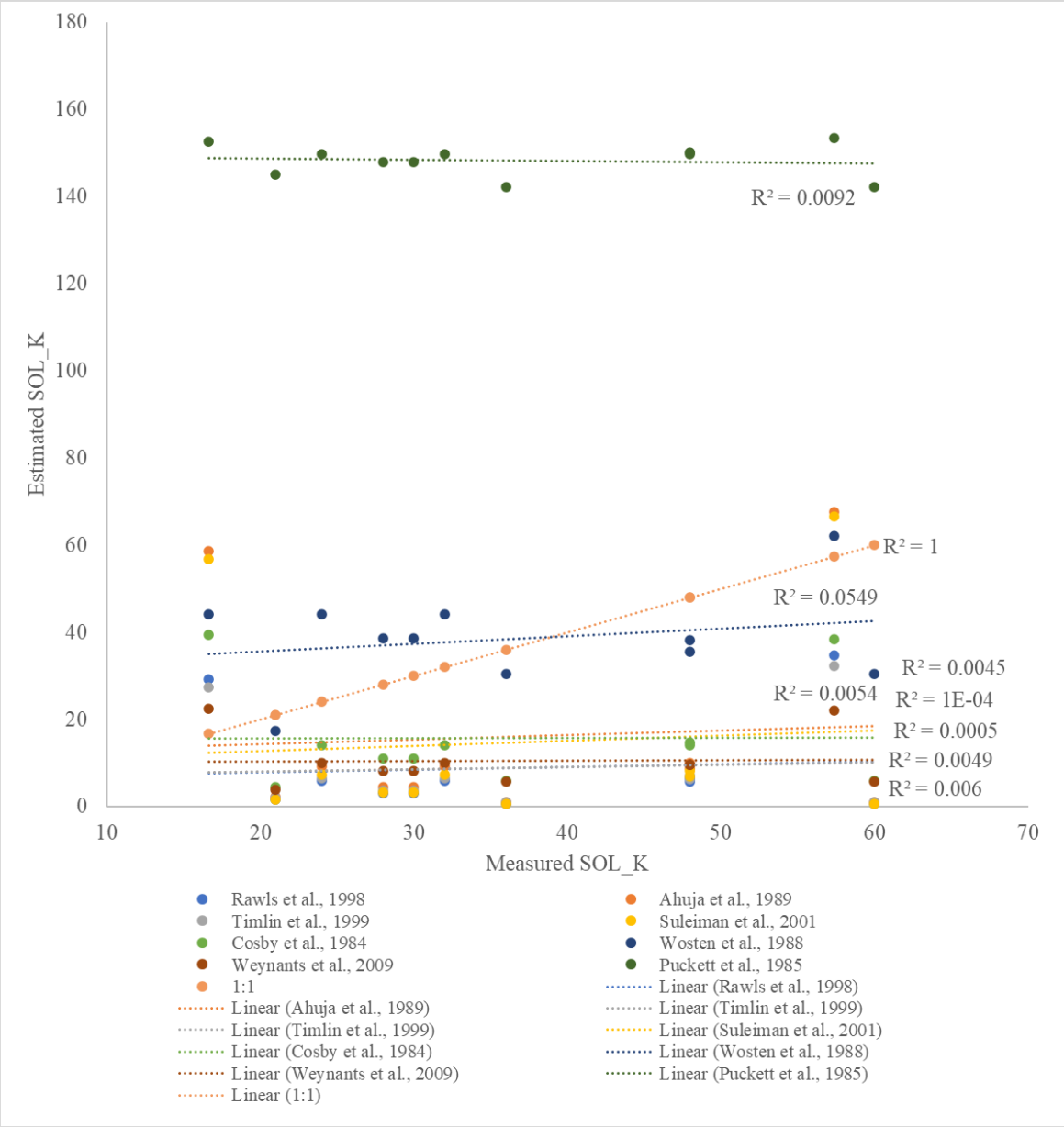

Figure 4.5 Scattered plot of predicted and actual SOL_K in Clear Creek watershed

Table 4. 7 Statistical performances of nine published PTFs in terms of R^2 and RMSE

PTF	Statistical measure			
	Cypress Creek		Clear Creek	
	R^2	RMSE	R^2	RMSE
Rawls et al., 1998	0.37	45.00	0.01	31.21
Ahuja et al., 1989	0.44	41.09	0.00	31.44
Timlin et al., 1999	0.36	47.53	0.00	30.91
Suleiman et al., 2001	0.45	43.41	0.01	32.07
Cosby et al., 1984	0.51	43.42	0.00	26.34
Wosten et al., 1988	0.66	29.82	0.05	14.99
Weynants et al., 2009	0.55	55.42	0.00	28.74
Saxton et al., 1986	0.13	45.89	0.02	287.62
Puckett et al., 1985	0.02	107.73	0.01	107.99

4.4 Development and evaluation of a new pedotransfer function

4.4.1 Correlation Analysis

Based on the previous studies, the possible appropriate predictors for SOL_K were chosen as soil texture (SD, CL, and SI), soil organic matter (OM), and SRL. In early studies, SOL_K was predicted based on soil texture (Ahuja et al., 1985; Clapp and Hornberger, 1978; Rawls et al., 1998). Later, OM was included to improve the prediction of SOL_K (Rawls et al., 2004; Saxton and Rawls, 2006). Recently, many studies

incorporated additional variables such as salinity, topography, and vegetation to enhance the SOL_K prediction which can be applied for specific land use (Jana and Mohanty, 2011; Leij et al., 2004; Pachepsky et al., 2001; Yao et al., 2015). From our finding, the correlation among SOL_K, soil texture, OM, and SRL was significant for the pairs of OM-CL, OM-SI, OM-SD, OM-SOL_K, CL-SD, SOL_K-SI, SOL_K-SD, and SOL_K-SRL at alpha 0.05 (Table 4.4). The Pearson correlation coefficient (r) for SOL_K-SRL was 0.65 indicating a 65% positive relationship between SOL_K and SRL. Higher SRL is related to the finer fibrous root system. The correlation coefficient between OM-SRL was -0.29, which is a negative correlation and was not significant. Fine roots have more contact with soil microorganisms, and less lignin content resulted in high decomposition, and produces soil organic matter (Poirier et al., 2018), which increases SOL_K; however, the correlation between SRL and decomposition is not consistent among various species (Poirier et al., 2018; Roumet et al., 2016). SOL_K had strong positive correlation with soil texture (r = 0.67) than SRL (r= 0.64) and OM (r= -0.6).

Table 4. 8 Pearson correlation coefficients and Pr>|r| among SOL_K, SRL, OM and soil texture (CL, SI, and SD)

	OM	CL	SI	SD	SRL
CL	0.8477				
	0.0005				
SI	0.6658	0.313			
	0.0181	0.3219			
	-0.83354	-0.57707	-0.95628		

SD	0.0008	0.0495	<.0001		
SRL	-0.28893	0.06037	-0.48838	0.40137	
	0.3624	0.8522	0.1072	0.1959	
SOL_K	-0.60046	-0.12737	-0.73358	0.67003	0.64872
	0.039	0.6932	0.0066	0.0171	0.0225

4.4.2 Multiple linear regression (MLR)

The stepwise multiple linear regression analysis provided the accurate prediction of SOL_K when using SD and SRL as predictors. However, the equation was reanalyzed, and SI and OC were added to make the equation applicable for all textural classes of native prairie soils. The developed equation to predict SOL_K was found to be as follows:

$$SOL\_K = 3.97670 * SI - 1.684947 * OC + 16.207563 * SD * SRL \quad (19)$$

Where SOL_K is saturated hydraulic conductivity in mm/hr, SI is the proportion of silt content (e.g., 80% of clay is denoted as 0.8), OC is the proportion of organic carbon content to soil weight, SD is the proportion of sand content, and SRL is the specific root length in m/g.

Results of the analysis of variance showed that SOL_K has a significant linear effect on the multiplication of SD and SRL ($P < 0.0001$). R^2 was 0.9226, indicating that 92% of the variation of SOL_K could be explained by SI, OC, SD, and SRL in the regression model. RMSE was 21.16. The developed equation was validated with measured SOL_K at the Clear Creek Watershed with an R^2 of 0.21. Two independent

sample t-test using SAS were performed. Results showed a variance of two SOL_Ks of measured and estimated by new PTF were equal (P=0.4125) at alpha 0.5. There was no significant difference between the mean of measured SOL_K and the mean of estimated SOL_K at Clear Creek at alpha 0.1 (P=0.6220).

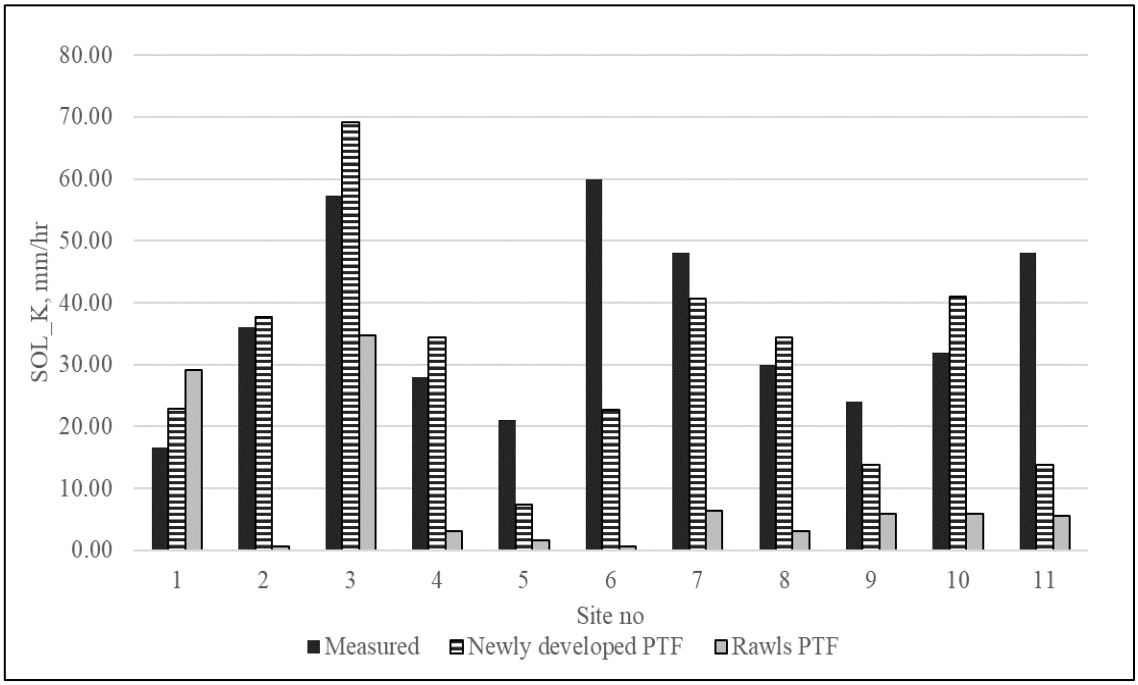

Figure 4.6 Comparison of SOL_K from field measurement, by using newly developed PTF, and by using PTF by Rawls et al. (1998) at Clear Creek watershed

Figure 4.6 showed measured SOL_K and estimated SOL_K by Rawls equation and newly developed equation at 11 test sites in Clear Creek. As expected, the developed PTF had the best prediction of SOL_K compared to the Rawls et al. (1998) PTF (Figure 4.5) due to the inclusion of SRL. Higher SRL enhance the soil structure and increase the soil aggregates. Fine roots and hairs closely attach to the soil particles and contribute to the accumulation of soil organic carbon (Poirier et al., 2018). The newly developed equation might not be accurate for conditions that are greatly different from the soils it

was developed for. It is observed that SOL_K in prairie soil tend to increase with clay percent whereas in general clay particles restricts the infiltration. The possible reason for this effect would be root penetration in the clay soil attribute to cracks and provide pathway for water infiltration; however, root penetration in sandy particles may not create cracks.

Rawls's PTF is a widely used equation to predict SOL_K (Patil and Singh, 2016; Saxton and Rawls, 2006). However, SOL_K was underpredicted when applying Rawls's PTF in native prairie soils except for site 1 (Figure 4.5). At site 2 (native prairie land), measured SOL_K were observed to be more than 40 mm/hr. Rawls PTF estimated SOL_K with soil texture where sand content was lower in site 2 and 6 (Figure 4) which was the more sensitive variable (Table 3). Therefore, Rawls's PTF underpredicted SOL_K in prairie lands. The inclusion of SRL in the equation enhanced the SOL_K prediction in all prairie sites. Specifically, sites 2 and 6 have vegetation of king ranch bluestem, little bluestem, and Bermuda grass (Table 4.2). The inclusion of the average SRL of that vegetation in the new PTF enhanced the prediction well in site 2. However, in site 6, 7, and 11 the prediction from new equation is still underestimating SOL_K. The effect of clay soil cracks due to the root penetration should be included to enhance the PTF further. Site 5 is the grassland nearby the sports park at Sanger. It also has the potential for soil compaction. Site 8 is native prairie land; however, weeds (rag weeds) were observed in the field. That might have resulted in overprediction of SRL. Studies showed that SRL does not have positive correlation with soil aggregation all the time; it all depends on the plant type (Poirier et al., 2018).

4.5 Evaluating the impact of newly developed pedotransfer function on the calibration of SWAT model

4.5.1 Distribution of soil hydraulic conductivity (SOL_Ks)

The calibrated and estimated SOL_K at each HRUs were tabulated in Appendix A. During the calibration, SOL_K adjustment was done relative to the initial values. Initially the model has assigned SOL_K values based on the soil texture class data. Thus, calibrated values resulted in similar results for the same texture classes regardless of land use. For example, calibrated SOL_Ks were the same for the soil texture class of fine sandy loam; however, SOL_Ks from the new PTF vary within the fine sandy loam class as a result of the integration of SRL into the equation. Figure 4.7 shows the heterogeneous nature of SOL_K using the newly developed PTF as compared to the other two methods.

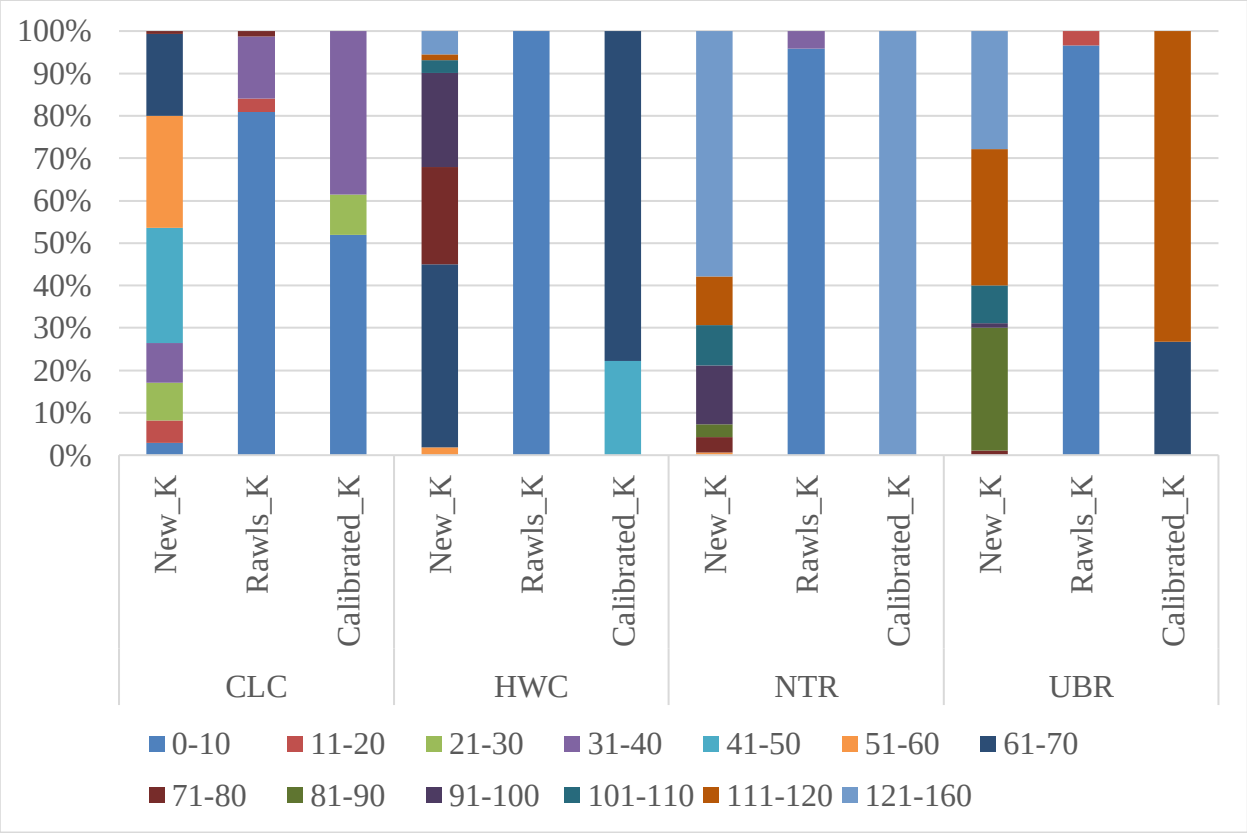

Figure 4.7 Distribution of SOL_Ks resulting from the three methods (New PTF, Rawls PTF, and Calibrated) in the HRUs for the four watersheds

4.5.2 Model performances

Model performances were evaluated and compared for each simulation. The application of the new PTF in the model slightly improved the model performance (Table 4. 9). The SOL_Ks from the new PTF were added in the calibrated model, and simulations were compared against observed streamflow. The statistical measure of RSR and NSE seemed to result in improvement for all watersheds, whereas PBIAS only improved for a few events. During the calibration, SOL_K was adjusted based on the initial assignment without affecting its heterogeneous nature. In real field conditions, the SOL_K of native prairie soils is highly variable temporarily and spatially (Chandrasoma

et al., 2016; Mohanty and Zhu, 2007). In this study, calibrated SOL_K were observed to be more homogenous, and SOL_Ks from the newly developed PTF were more heterogeneous (Figure 4.7).

In addition, SRL in the new equation resulted in an improved estimation of SOL_K where SOL_Ks were underestimated as compared to the Rawls PTF. The heterogeneous nature of SOL_K and the inclusion of characteristics of root improve the SOL_K estimation. Thus, the model simulations of the flow matched well with the observed flow.

Table 4. 9 Model performance results with rating according to Moriasi et al., 2007

Watershed	RSR		NSE		PBIAS	
	Calibrated	New_PTF	Calibrated	New_PTF	Calibrated	New_PTF
CLC	0.60	0.51	0.63	0.74	-0.37	27.16
	Sat	Good	Sat	Good	V Good	Unsat
HWC	0.59	0.60	0.65	0.63	43.20	53.45
	Good	Sat	Sat	Sat	Unsat	Unsat
NTR	0.67	0.65	0.54	0.57	-15.68	38.89
	Sat	Sat	Sat	Sat	Sat	Unsat
UBR	0.60	0.60	0.63	0.63	15.08	15.12
	Sat	Sat	Sat	Sat	Good	Good

CHAPTER V

SUMMARY AND CONCLUSION

5.1 Summary

This research study focuses on developing a pedotransfer function that can be applied to native prairie soils. Native prairie soils are structurally different from similar texture non-prairie soils as native prairie soils are rich in prairie vegetation root systems which penetrate well into the soil profile. Mechanical binding of prairie root systems creates air-dry soil aggregates and produces higher soil organic matter. These structural changes influence the soil hydraulic properties. Watersheds with dominant land-use of prairie lands were modeled using SWAT, and calibrated soil parameters were compared with soil parameters calculated with commonly used Rawls PTF. The potential error resulting from using Rawls et al. (1998) PTF applied for native prairie soils was evaluated. The results proved that there is a gap that need to be bridged in Rawls PTF when modeling native prairie soils. A new PTF equation was developed using multiple linear regression. The incorporation of root characteristics in addition to soil texture and soil organic matter in the development of the PTF improved the estimation of hydraulic conductivity of native prairie soils. The new predictor called specific root length (SRL) was added in the new PTF to represent the root characteristics. The new PTF was integrated into the SWAT model, and the results of the simulations were analyzed compared to calibrated values and Rawls PTF values.

5.2 Conclusions

From this study, a new pedotransfer function was developed to include root characteristics to estimate the hydraulic conductivity of native prairie soil. The new pedotransfer function estimates native soil hydraulic conductivity accurately, which can be used to modeling

studies and other research study of native prairie soils. The newly developed equation was evaluated with R^2 of 0.92 and validated with R^2 of 0.21 which is better than the values obtained with Rawls equation (Figure 4.4).

The following conclusions were drawn from this study:

1. Analysis of SWAT model calibrated soil parameters
    a. The SWAT model calibrated soil parameters of native prairie soils (saturated hydraulic conductivity, soil available water content, and soil bulk density) are significantly different from calculated soil parameters by the PTF of Rawls et al. 1998.
    b. The SWAT model calibrated soil parameters are homogenous (i.e., similar values are given to the same soil textural classes), and soil parameters from Rawls et al. (1998) are heterogeneous across the watershed (i.e., values vary within the same textural class).
2. Analysis of potential deficiency
    a. The accuracy of nine existing PTFs in predicting SOL_K proved to be unsatisfactory based on the coefficient of determination (R^2) and RMSE (Root means squared error).
    b. The existing PTFs with soil texture, soil organic carbon, and soil density as independent variables estimate better than the existing PTF with a single independent variable, when applied in native prairie soils
    c. Use of soil texture, soil organic matter only as the independent variables in the existing PTFs results in failure to accurately predict the hydraulic properties of native prairie soils

3. Development of a new PTF
    a. The percentage of sand and specific root length are the most sensitive independent variables for estimating SOL_K of native prairie soil. However, the addition of more independent variables in the PTF to make it applicable for extended native prairie soils.
    b. The incorporation of specific root length (SRL) as an independent variable (predictor) in the newly developed PTF showed a better prediction of SOL_K of native prairie soils
4. Evaluation of the newly developed PTF
    a. The newly developed PTF estimates higher and more accurate SOL_K compared to the SOL_K underestimated by the Rawls et al. (1998) PTF. It indicated incorporation of SRL improves the estimation.
    b. The means of SOL_K estimated by the newly developed PTF were comparable with SWAT calibrated SOL_Ks for the four watersheds.
    c. The estimated SOL_K by the newly developed PTF was more heterogeneous (varied within one soil textural class) across the watershed compared to the calibrated SOL_K.
    d. The SWAT model, with the integration of the newly developed PTF, performed well in four watersheds with prairie land as major land-use across the Great Plains as demonstrated by goodness-of-fit statistical measures such as Nash-Sutcliffe Efficiency, root mean square Standard deviation Ratio, and percent bias.

5.3 Future work

The new PTF has been developed in this study incorporating root characteristics (specific

root length) with limited field measured data at Cypress Creek watershed. A larger measured dataset that includes laboratory data, would give even more accurate estimates for parameters in the equation. In this study, we used stepwise multiple linear regression method to develop the equation. The PTFs can be developed using an artificial neural network, which may result in a more accurate estimation. Also, in this study, only one independent variable (SRL) was added in addition to other common independent variable for SOL_K. However, many factors can significantly affect the SOL_K, such as tillage, grazing, weeds, and wormholes. The development of an equation that addresses those factors may increase the accuracy of estimation.

REFERENCES

Adams, W. A. 1973. The Effect of Organic Matter on the Bulk and True Densities of Some Uncultivated Podzolic Soils. *Journal of Soil Science* 24(1):10-17.

Ahmad, Z., F. Nadeem, R. Wang, X. Diao, Y. Han, X. Wang, and X. Li. 2018. A Larger Root System Is Coupled With Contrasting Expression Patterns of Phosphate and Nitrate Transporters in Foxtail Millet [Setaria italica (L.) Beauv.] Under Phosphate Limitation. 9(1367).

Ahuja, L. R., D. K. Cassel, R. R. Bruce, and B. B. Barnes. 1989. Evaluation of Spatial Distribution of Hydraulic Conductivity Using Effective Porosity Data. *Soil Science* 148(6).

Ahuja, L. R., J. W. Naney, and R. D. Williams. 1985. Estimating Soil Water Characteristics from Simpler Properties or Limited Data. *Soil Science Society of America journal* 49(5):1100-1105.

Aimrun, W., and M. S. M. Amin. 2009. Pedo-transfer function for saturated hydraulic conductivity of lowland paddy soils. *Paddy and Water Environment* 7(3):217-225.

Alexander, E. B. 1980. Bulk Densities of California Soils in Relation to Other Soil Properties. 44(4):689-692.

Arnold, J. G., J. R. Kiniry, R. Srinivasan, J. R. Wiiliams, E. B. Haney, and S. L. Neitsch.2012a.SWAT Mannual. College Station, TX: Texas Water Resource Institute.

Arnold, J. G., D. N. Moriasi, P. W. Gassman, K. C. Abbaspour, M. J. White, R. Srinivasan, C. Santhi, R. D. Harmel, A. van Griensven, M. W. Van Liew, N. Kannan, and M. K. Jha. 2012b. SWAT: Model Use, Calibration, and Validation. *Transactions of the ASABE* 55(4):1491-1508.

Bayabil, H. K., Y. T. Dile, T. Y. Tebebu, T. A. Engda, and T. S. Steenhuis. 2019. Evaluating infiltration models and pedotransfer functions: Implications for hydrologic modeling. *Geoderma* 338:159-169.

Berz, G., W. Kron, T. Loster, E. Rauch, J. Schimetschek, J. Schmieder, A. Siebert, A. Smolka, and A. Wirtz. 2001. World Map of Natural Hazards – A Global View of the Distribution and Intensity of Significant Exposures. *Natural Hazards* 23(2):443-465.

Bharati, L., K. H. Lee, T. M. Isenhart, and R. Schultz. 2002. Soil-Water Infiltration Under Crops, Pasture, and Established Riparian Buffer in Midwestern USA. *Agroforestry Systems* 56:249-257.

Blanco-Canqui, H., B. Wienhold, V. Jin, M. Schmer, and L. Kibet. 2017. Long-term tillage impact on soil hydraulic properties. *Soil and Tillage Research* 170:38-42.

Bo, X., and J. David. 2019. Morphological and Physiological Responses of Seashore Paspalum and Bermudagrass to Waterlogging Stress. *Journal of the American Society for Horticultural Science J. Amer. Soc. Hort. Sci.* 144(5):305-313.

Bouma, J. 1989. Using Soil Survey Data for Quantitative Land Evaluation. In *Advances in Soil Science: Volume 9*, 177-213. B. A. Stewart, ed. New York, NY: Springer US.

Briggs, L. J., and H. L. Shantz. 1912. The Wilting Coefficient and Its Indirect Determination. *Botanical Gazette* 53(1):20-37.

Brooks, R. H., and A. T. Corey. 1964. *Hydraulic Properties of Porous Media*. Colorado State University.

Brye, K. R., and T. L. Riley. 2009. Soil and Plant Property Differences Across a Chronosequence of Humid-Temperate Tallgrass Prairie Restorations. *Soil Science* 174(6).

Burke, I. C., C. M. Yonker, W. J. Parton, C. V. Cole, K. Flach, and D. S. Schimel. 1989. Texture, Climate, and Cultivation Effects on Soil Organic Matter Content in U.S. Grassland Soils. 53(3):800-805.

Chandrasoma, J. M., R. P. Udawatta, S. H. Anderson, A. L. Thompson, and M. A. Abney. 2016. Soil hydraulic properties as influenced by prairie restoration. *Geoderma* 283:48-56.

Chen, X., J. Zhang, Y. Chen, Q. Li, F. Chen, L. Yuan, and G. Mi. 2014. Changes in root size and distribution in relation to nitrogen accumulation during maize breeding in China. *Plant and Soil* 374(1):121-130.

Chicco, D., M. J. Warrens, and G. Jurman. 2021. The coefficient of determination R-squared is more informative than SMAPE, MAE, MAPE, MSE and RMSE in regression analysis evaluation. *PeerJ Comput Sci* 7:e623.

Clapp, R. B., and G. M. Hornberger. 1978. Empirical equations for some soil hydraulic properties. *Water Resources Research* 14(4):601-604.

Coleman, D. C., J. M. Oades, and G. Uehara. 1989. Dynamics of soil organic matter in tropical ecosystems.

Comas, L. H., H. S. Callahan, and P. E. Midford. 2014. Patterns in root traits of woody species hosting arbuscular and ectomycorrhizas: implications for the evolution of belowground strategies. *Ecology and evolution* 4(15):2979-2990.

Cornelis, W. M., J. Ronsyn, M. Van Meirvenne, and R. Hartmann. 2001. Evaluation of Pedotransfer Functions for Predicting the Soil Moisture Retention Curve. *Soil Science Society of America journal* 65(3):638-648.

Cosby, B. J., G. M. Hornberger, R. B. Clapp, and T. R. Ginn. 1984. A Statistical Exploration of the Relationships of Soil Moisture Characteristics to the Physical Properties of Soils. *Water Resources Research* 20(6):682-690.

Cowdery, T. K., C. A. Christenson, and J. R. Ziegeweid. 2019. The hydrologic benefits of wetland and prairie restoration in western Minnesota—Lessons learned at the Glacial Ridge National Wildlife Refuge, 2002–15. Reston, VA: U. S. G. Survey.

Craine, J. M., D. A. Wedin, F. S. Chapin, and P. B. Reich. 2003. Relationship between the structure of root systems and resource use for 11 North American grassland plants. *Plant Ecology* 165(1):85-100.

Curtis, R. O., and B. W. Post. 1964. Estimating Bulk Density from Organic-Matter Content in Some Vermont Forest Soils. 28(2):285-286.

EPA. 2021. Ecoregions of North America. Washington, DC 20460. Available at: https://www.epa.gov/eco-research/ecoregions-north-america.

Fernández, M. C., H. Belinque, F. H. G. Boem, and G. Rubio. 2009. Compared Phosphorus Efficiency in Soybean, Sunflower and Maize. *Journal of Plant Nutrition* 32(12):2027-2043.

Feyereisen, G. W., T. Strickland, D. Bosch, and D. G. Sullivan. 2007. Evaluation of SWAT Manual Calibration Sensitivity in the Little River Watershed. *Transactions of the ASABE* 50.

Fuentealba, M., J. Zhang, K. Kenworthy, J. Erickson, J. Kruse, and L. Trenholm. 2015. Root Development and Profile Characteristics of Bermudagrass and Zoysiagrass. *HortScience: a publication of the American Society for Horticultural Science* 50:1429-1434.

Fuentes, J. P., M. Flury, and D. F. Bezdicek. 2004. Hydraulic Properties in a Silt Loam Soil under Natural Prairie, Conventional Till, and No-Till. 68(5):1679-1688.

Gerla, P. J., M. W. Cornett, J. D. Ekstein, and M. A. Ahlering. 2012. Talking Big: Lessons Learned from a 9000 Hectare Restoration in the Northern Tallgrass Prairie. 4(11):3066-3087.

Grace, J. B., L. K. Allain, and C. Allen. 2000. Factors associated with plant species richness in a coastal tall-grass prairie. *Journal of Vegetation Science* 11(3):443-452.

Gu, D., F. Zhen, D. B. Hannaway, Y. Zhu, L. Liu, W. Cao, and L. Tang. 2017. Quantitative Classification of Rice (Oryza sativa L.) Root Length and Diameter Using Image Analysis. *PLOS ONE* 12(1):e0169968.

Guo, J., H.-Y. Li, L. R. Leung, S. Guo, P. Liu, and M. Sivapalan. 2014. Links between flood frequency and annual water balance behaviors: A basis for similarity and regionalization. *Water Resources Research* 50(2):937-953.

H. Gowda, P., D. J. Mulla, E. D. Desmond, A. D. Ward, and D. N. Moriasi. 2012. ADAPT: Model Use, Calibration, and Validation. *Transactions of the ASABE* 55(4):1345-1352.

H. Jaber, F., and S. Shukla. 2012. MIKE SHE: Model Use, Calibration, and Validation. *Transactions of the ASABE* 55(4):1479-1489.

Harris County Flood Control Disrict. 2021. Flood damage reduction tools. Houston, TX: Harris County Flood Control Disrict. Available at: https://www.hcfcd.org/About/Flood-Damage-Reduction-Tools.

Harris County Flood Warning System. 2020. Sub-daily rainfall data. Harris County Flood Control Disrict, ed.

Haukos, J. 2014. The Tallgrass Paririe History. Kansas.

Herkes, D. M. G., A. Gori, and A. Juan. 2017. Impact of Prairie Cover on Hydraulic Conductivity and Storm Water Runoff.

Hernandez-Santana, V., X. Zhou, M. J. Helmers, H. Asbjornsen, R. Kolka, and M. Tomer. 2013. Native prairie filter strips reduce runoff from hillslopes under annual row-crop systems in Iowa, USA. *Journal of Hydrology* 477:94-103.

Hillel, D. 2003. 1 - Soil Physics and Soil Physical Characteristics. In *Introduction to Environmental Soil Physics*, 3-17. D. Hillel, ed. Burlington: Academic Press.

Hirmas, D. R., and R. D. Mandel. 2017. Soils of the Great Plains. In *The Soils of the USA*, 131-163. L. T. West, M. J. Singer, and A. E. Hartemink, eds. Cham: Springer International Publishing.

Huf Dos Reis, A. M., R. A. Armindo, M. F. Durães, and Q. De Jong Van Lier. 2018. Evaluating pedotransfer functions of the Splintex model. 69(4):685-697.

Huntington, T. G., C. E. Johnson, A. H. Johnson, T. G. Siccama, and D. F. Ryan. 1989. Carbon, organic matter, and bulk density relationships in a forested spodosol. *Soil Science* 148(5).

Jana, R. B., and B. P. Mohanty. 2011. Enhancing PTFs with remotely sensed data for multi-scale soil water retention estimation. *Journal of Hydrology* 399(3):201-211.

Jha, M. K. 2011. Evaluating Hydrologic Response of an Agricultural Watershed for Watershed Analysis. *Water* 3(2).

Kalam, S., A. Basu, I. Ahmad, R. Z. Sayyed, H. A. El-Enshasy, D. J. Dailin, and N. L. Suriani. 2020. Recent Understanding of Soil Acidobacteria and Their Ecological Significance: A Critical Review. 11(2712).

Kätterer, T., O. Andrén, and P. E. Jansson. 2006. Pedotransfer functions for estimating plant available water and bulk density in Swedish agricultural soils. *Acta Agriculturae Scandinavica, Section B — Soil & Plant Science* 56(4):263-276.

Kay, B. D. 1990. Rates of Change of Soil Structure Under Different Cropping Systems. In *Advances in Soil Science 12: Volume 12*, 1-52. B. A. Stewart, ed. New York, NY: Springer New York.

Kharel, G., H. Zheng, and A. Kirilenko. 2016. Can land-use change mitigate long-term flood risks in the Prairie Pothole Region? The case of Devils Lake, North Dakota, USA. *Regional Environmental Change* 16(8):2443-2456.

Kirkham, M. B. 2005. 7 - Water Movement in Saturated Soil. In *Principles of Soil and Plant Water Relations*, 85-100. M. B. Kirkham, ed. Burlington: Academic Press.

Larson, D. L., J. B. Bright, P. Drobney, J. L. Larson, and S. Vacek. 2017. Persistence of native and exotic plants 10 years after prairie reconstruction. *Restoration Ecology* 25(6):953-961.

Lauenroth, W., D. Schlaepfer, and J. Bradford. 2014. Ecohydrology of Dry Regions: Storage versus Pulse Soil Water Dynamics. *Ecosystems* 17(8):1469-1479.

Leij, F., N. Romano, M. Palladino, M. Schaap, and A. Coppola. 2004. Topographic attributes to predict soil hydraulic properties along a hillslope transect. *Water Resources Research* 40, W02407:1-15.

Lenhart, T., K. Eckhardt, N. Fohrer, and H. G. Frede. 2002. Comparison of two different approaches of sensitivity analysis. *Physics and Chemistry of the Earth, Parts A/B/C* 27(9):645-654.

Leuschner, C., D. Hertel, I. Schmid, O. Koch, A. Muhs, and D. Hölscher. 2004. Stand fine root biomass and fine root morphology in old-growth beech forests as a function of precipitation and soil fertility. *Plant and Soil* 258(1/2):43-56.

Li, S., Q. Zuo, X. Wang, W. Ma, X. Jin, J. Shi, and A. Ben-Gal. 2017. Characterizing roots and water uptake in a ground cover rice production system. *PLOS ONE* 12(7):e0180713.

Low, A. J. 1972. The Effect of Cultivation on the Structure and Other Physical Characteristics of Grassland and Arable Soils *European Journal of Soil Science* 23(4):363-380.

Lu, J., Q. Zhang, A. D. Werner, Y. Li, S. Jiang, and Z. Tan. 2020. Root-induced changes of soil hydraulic properties – A review. *Journal of Hydrology* 589:125203.

Lyu, Y., H. Tang, H. Li, F. Zhang, Z. Rengel, W. R. Whalley, and J. Shen. 2016. Major Crop Species Show Differential Balance between Root Morphological and Physiological Responses to Variable Phosphorus Supply. 7(1939).

Maguire, D. J. 2008. ArcGIS: General Purpose GIS Software System. In *Encyclopedia of GIS*, 25-31. S. Shekhar, and H. Xiong, eds. Boston, MA: Springer US.

Malone, R. W., Y. Gene, C. Baffaut, M. Gitau, Z. Qi, D. M. Amatya, P. Parajuli, V. James, and T. Green. 2015. Parameterization Guidelines and Considerations for Hydrologic Models. *Transactions of the ASABE (American Society of Agricultural and Biological Engineers)* 58.

Mazurak, A. P., and R. E. Ramig. 1962. Aggregation and Air-Water Permeabilities in a Chernozem Soil Cropped to Perennial Grasses and Fallow-Grain. *Journal of Soil Science* 94(3):151-157.

Merdun, H., Ö. Çınar, R. Meral, and M. Apan. 2006. Comparison of artificial neural network and regression pedotransfer functions for prediction of soil water retention and saturated hydraulic conductivity. *Soil and Tillage Research* 90(1):108-116.

Mohanty, B. P., and J. Zhu. 2007. Effective Hydraulic Parameters in Horizontally and Vertically Heterogeneous Soils for Steady-State Land?Atmosphere Interaction. *Journal of Hydrometeorology* 8(4):715-729.

Moriasi, D. N., J. G. Arnold, M. W. Van Liew, R. L. Bingner, R. D. Harmel, and T. L. Veith. 2007. Model Evaluation Guidelines for Systematic Quantification of Accuracy in Watershed Simulations. *Transactions of the ASABE* 50(3):885-900.

Murphy, C., B. Foster, M. Ramspott, and K. Price. 2009. Grassland management and soil bulk density. *Transactions of the Kansas Academy of Science* 107:45-54.

Nearing, M. A., B. Y. Liu, L. M. Risse, and X. Zhang. 1996. Curve Numbers and Green-Ampt Effective Hydraulic Conductivities. *JAWRA Journal of the American Water Resources Association* 32(1):125-136.

Neitsch, S. L., J. G. Arnold, J. R. Kiniry, and J. R. Williams. 2009. Soil and Water Assessment Tool Theoretical Documentation Version 2009. T. W. R. Institute, ed. College Station, TX: Grassland, Soil and Water Research Laboratory, Agricultural Research Service

Blackland Research Center, Texas Agricultural Experiment Station.

Nemes, A., W. J. Rawls, and Y. A. Pachepsky. 2005. Influence of Organic Matter on the Estimation of Saturated Hydraulic Conductivity. *Soil Science Society of America journal* 69(4):1330-1337.

NOAA National Centers for Environmental Information (NCEI). 2005. U.S. Hourly Precipitation Data. U.S. Department of Commerce, ed.

Obi, J. C., P. I. Ogban, U. J. Ituen, and B. T. Udoh. 2014. Development of pedotransfer functions for coastal plain soils using terrain attributes. *CATENA* 123:252-262.

Ostonen, I., Ü. Püttsepp, C. Biel, O. Alberton, M. R. Bakker, K. Lõhmus, H. Majdi, D. Metcalfe, A. F. M. Olsthoorn, A. Pronk, E. Vanguelova, M. Weih, and I. Brunner. 2007. Specific root length as an indicator of environmental change. *Plant Biosystems - An International Journal Dealing with all Aspects of Plant Biology* 141(3):426-442.

Pachepsky, Y., D. Timlin, and W. J. Rawls. 2001. Soil Water Retention as Related to Topographic Variables. *Soil Sci. Soc. Am. J.* 65.

Pachepsky, Y. A., and W. J. Rawls. 1999. Accuracy and Reliability of Pedotransfer Functions as Affected by Grouping Soils. *Soil Science Society of America journal* 63(6):1748-1757.

Pang, J., M. H. Ryan, M. Tibbett, G. R. Cawthray, K. H. M. Siddique, M. D. A. Bolland, M. D. Denton, and H. Lambers. 2010. Variation in morphological and physiological parameters in herbaceous perennial legumes in response to phosphorus supply. *Plant and Soil* 331(1):241-255.

Patil, N. G., and S. K. Singh. 2016. Pedotransfer Functions for Estimating Soil Hydraulic Properties: A Review. *Pedosphere* 26(4):417-430.

Poirier, V., C. Roumet, and A. D. Munson. 2018. The root of the matter: Linking root traits and soil organic matter stabilization processes. *Soil Biology and Biochemistry* 120:246-259.

Puckett, W. E., J. H. Dane, and B. F. Hajek. 1985. Physical and Mineralogical Data to Determine Soil Hydraulic Properties. *Soil Science Society of America journal* 49(4):831-836.

Purakayastha, T. J., D. R. Huggins, and J. L. Smith. 2008. Carbon Sequestration in Native Prairie, Perennial Grass, No-Till, and Cultivated Palouse Silt Loam. *Soil Science Society of America journal* 72(2):534-540.

Qiao, J., Y. Zhu, X. Jia, L. Huang, and M. a. Shao. 2018. Development of pedotransfer functions for soil hydraulic properties in the critical zone on the Loess Plateau, China. *Hydrological Processes* 32(18):2915-2921.

Ranjitkumar, M., T. Meenambal, and V. Kumar. 2015. Pedotransfer Functions in Hydrologic Modelling for Predicting the Effect of Chnages in Soil Types on Watershed Hydrology. *International Journal of Earth Sciences and Engineering* 8(2):201-211.

Rawls, W. J. 1983. Estimating soil bulk density from particle size analysis and organic matter content1. *Soil Science* 135(2).

Rawls, W. J., D. L. Brakensiek, and K. E. Saxtonn. 1982. Estimation of Soil Water Properties. *Transactions of the ASAE* 25(5):1316-1320.

Rawls, W. J., D. Gimenez, and R. Grossman. 1998. Use of soil texture, bulk density, and slope of the water retention curve to predict saturated hydraulic conductivity. *Transactions of the ASAE* 41(4):983-988.

Rawls, W. J., A. Nemes, and Y. Pachepsky. 2004. Effect of soil organic carbon on soil hydraulic properties. In *Developments in Soil Science*, 95-114. Elsevier.

Rawls, W. J., Y. A. Pachepsky, J. C. Ritchie, T. M. Sobecki, and H. Bloodworth. 2003. Effect of soil organic carbon on soil water retention. *Geoderma* 116(1):61-76.

Rebecca Nelson, B., P. Cynthia, N. Sophia, and D. Samantha. 2010. Relative Rooting Depths of Native Grasses and Amenity Grasses with Potential for Use on Roadsides in New England. *HortScience horts* 45(3):393-400.

Rezaei, M., T. Saey, P. Seuntjens, I. Joris, W. Boënne, M. Van Meirvenne, and W. Cornelis. 2016. Predicting saturated hydraulic conductivity in a sandy grassland using proximally sensed apparent electrical conductivity. *Journal of Applied Geophysics* 126:35-41.

Rosenzweig, S. T., M. A. Carson, S. G. Baer, and J. M. Blair. 2016. Changes in soil properties, microbial biomass, and fluxes of C and N in soil following post-agricultural grassland restoration. *Applied Soil Ecology* 100:186-194.

Roumet, C., M. Birouste, C. Picon-Cochard, M. Ghestem, N. Osman, S. Vrignon-Brenas, K.-f. Cao, and A. Stokes. 2016. Root structure–function relationships in 74 species: evidence of a root economics spectrum related to carbon economy. *New Phytologist* 210(3):815-826.

Samson, F., and F. Knopf. 1994. Prairie conservation in North America. *BioScience* 44(6):418-421.

Saxton, K. E., and W. J. Rawls. 2006. Soil Water Characteristic Estimates by Texture and Organic Matter for Hydrologic Solutions. *Soil Science Society of America journal* v. 70(no. 5):pp. 1569-1560-2006 v.1570 no.1565.

Saxton, K. E., W. J. Rawls, J. S. Romberger, and R. I. Papendick. 1986. Estimating Generalized Soil-water Characteristics from Texture. 50(4):1031-1036.

Schaap, M. G., F. J. Leij, and M. T. van Genuchten. 1998. Neural Network Analysis for Hierarchical Prediction of Soil Hydraulic Properties. *Soil Science Society of America journal* 62(4):847-855.

Scharffenberg, W. 2016. Hydrologic Modeling System HEC-HMS User's Mannual. I. f. W. Resources, ed. Davis, CA: U.S Army Corps of Engineers.

Schwartz, R. C., S. R. Evett, and P. W. Unger. 2003. Soil hydraulic properties of cropland compared with reestablished and native grassland. *Geoderma* 116(1):47-60.

Sharma, S. K., B. P. Mohanty, and J. Zhu. 2006. Including Topography and Vegetation Attributes for Developing Pedotransfer Functions. *Soil Science Society of America journal* 70(5):1430-1440.

Singh, V. P. 1995. Watershed Modeling. In *Computer models of watershed hydrology. editor, Vijay P. Singh. Rev. ed.* V. P. Singh, ed: Water Resources Publications.

Soil Survey Staff. 2021. Soil Survey Geographic (SSURGO) Database. U. S. D. o. A. Natural Resources Conservation Service, ed.

Souza, T. C., P. Magalhães, E. M. Castro, V. P. Duarte, and A. J. P. A. B. Lavinsky. 2016. Corn root morphoanatomy at different development stages and yield under water stress. 51:330-339.

Suleiman, A., and J. Ritchie. 2001. Estimating Saturated Hydraulic Conductivity from Soil Porosity. *Transactions of the ASAE* 44.

Sun, W., X. Yao, N. Cao, Z. Xu, and J. Yu. 2016. Integration of soil hydraulic characteristics derived from pedotransfer functions into hydrological models: evaluation of its effects on simulation uncertainty. *Hydrology Research* 47(5):964-978.

Tamari, S., J. H. M. Wösten, and J. C. Ruiz-Suárez. 1996. Testing an Artificial Neural Network for Predicting Soil Hydraulic Conductivity. *Soil Science Society of America journal* 60(6):1732-1741.

Teepe, R., H. Dilling, and F. Beese. 2003. Estimating water retention curves of forest soils from soil texture and bulk density. *Journal of Plant Nutrition and Soil Science* 166(1):111-119.

Thompson, J. R. 1992. Praries, Forests, and Wetlands: The Restoration of Natural Landscape Communities in Lowa. Iowa, USA: University of Lowa Press.

Timlin, D. J., L. R. Ahuja, Y. Pachepsky, R. D. Williams, D. Gimenez, and W. Rawls. 1999. Use of Brooks-Corey Parameters to Improve Estimates of Saturated Conductivity from Effective Porosity. *Soil Science Society of America journal* 63(5):1086-1092.

Twarakavi, N. K. C., J. Šimůnek, and M. G. Schaap. 2009. Development of Pedotransfer Functions for Estimation of Soil Hydraulic Parameters using Support Vector Machines. *Soil Science Society of America journal* 73(5):1443-1452.

U.S. Geological Survey. 2019a. 3D Elevation Program 1/3 Arc Second Resolution Digital Elevation Model. U.S. Geological Survey, ed.

U.S. Geological Survey. 2019b. National Land Cover Database (NLCD) 2019 Land Cover Conterminous United States. U.S. Geological Survey, ed.

Udawatta, R. P., S. H. Anderson, C. J. Gantzer, and H. E. Garrett. 2008. Influence of Prairie Restoration on CT-Measured Soil Pore Characteristics. *Journal of Enviornmental Quality* 37(1):219-228.

van Genuchten, M. T. 1980. A Closed-form Equation for Predicting the Hydraulic Conductivity of Unsaturated Soils. *Soil Science Society of America journal* 44(5):892-898.

Van Looy, K., J. Bouma, M. Herbst, J. Koestel, B. Minasny, U. Mishra, C. Montzka, A. Nemes, Y. A. Pachepsky, J. Padarian, M. G. Schaap, B. Tóth, A. Verhoef, J. Vanderborght, M. J. van der Ploeg, L. Weihermüller, S. Zacharias, Y. Zhang, and H. Vereecken. 2017. Pedotransfer Functions in Earth System Science: Challenges and Perspectives. *Reviews of Geophysics* 55(4):1199-1256.

W. Gassman, P., M. R. Reyes, C. H. Green, and J. G. Arnold. 2007. The Soil and Water Assessment Tool: Historical Development, Applications, and Future Research Directions. *Transactions of the ASABE* 50(4):1211-1250.

W. Skaggs, R., M. A. Youssef, and G. M. Chescheir. 2012. DRAINMOD: Model Use, Calibration, and Validation. *Transactions of the ASABE* 55(4):1509-1522.

Wang, X., J. R. Williams, P. W. Gassman, C. Baffaut, R. C. Izaurralde, J. Jeong, and J. R. Kiniry. 2012. EPIC and APEX: Model Use, Calibration, and Validation. *Transactions of the ASABE* 55(4):1447-1462.

Weather data Library Kansas Mesonet. 2020. Sub-daily Precipitation K. S. University, ed.

Weaver, J. E. 1920. *Root development in the grassland formation : a correlation of the root systems of native vegetation and crop plants. by John E. Weaver*. Carnegie Institution of Washington publication: no. 292. Carnegie Institution of Washington.

Weaver, J. E. 1958. Summary and Interpretation of Underground Development in Natural Grassland Communities. *Ecological Monographs* 28(1):55-78.

Weaver, J. E. 1961. The Living Network in Prairie Soils. *Botanical Gazette* 123(1):16-28.

Weynants, M., H. Vereecken, and M. Javaux. 2009. Revisiting Vereecken Pedotransfer Functions: Introducing a Closed-Form Hydraulic Model. *Vadose zone journal* 8(1):86-95.

Wösten, J. H. M., A. Lilly, A. Nemes, and C. Le Bas. 1999. Development and use of a database of hydraulic properties of European soils. *Geoderma* 90(3):169-185.

Wösten, J. H. M., Y. A. Pachepsky, and W. J. Rawls. 2001. Pedotransfer functions: bridging the gap between available basic soil data and missing soil hydraulic characteristics. *Journal of Hydrology* 251(3):123-150.

Wösten, J. H. M., and M. T. van Genuchten. 1988. Using Texture and Other Soil Properties to Predict the Unsaturated Soil Hydraulic Functions. *Soil Science Society of America journal* 52(6):1762-1770.

Yang, W., X. Wang, Y. Liu, S. Gabor, L. Boychuk, and P. Badiou. 2010. Simulated environmental effects of wetland restoration scenarios in a typical Canadian prairie watershed. *Wetlands Ecology & Management* 18(3):269-279.

Yang, Z., B. Zhou, X. Ge, Y. Cao, I. Brunner, J. Shi, and M.-H. Li. 2021. Species-Specific Responses of Root Morphology of Three Co-existing Tree Species to Nutrient Patches Reflect Their Root Foraging Strategies. 11(2322).

Yao, R.-J., J.-S. Yang, D.-H. Wu, F.-R. Li, P. Gao, and X.-P. Wang. 2015. Evaluation of pedotransfer functions for estimating saturated hydraulic conductivity in coastal salt-affected mud farmland. *Journal of Soils and Sediments* 15(4):902.

Yu, Z. 2003. Hydrology | Modeling and Prediction. In *Encyclopedia of Atmospheric Sciences*, 980-987. J. R. Holton, ed. Oxford: Academic Press.

Zhang, H., H. Liu, D. Hou, Y. Zhou, M. Liu, Z. Wang, L. Liu, J. Gu, and J. Yang. 2019. The effect of integrative crop management on root growth and methane emission of paddy rice. *The Crop Journal* 7(4):444-457.

Zhang, Y., and M. G. Schaap. 2019. Estimation of saturated hydraulic conductivity with pedotransfer functions: A review. *Journal of Hydrology* 575:1011-1030.

APPENDIX A

INPUT VARIABLES FOR REGRESSION ANALYSIS

Cypress Creek							
Site name	**Soil Name**	**Location Lat/Long**	**Clay, %**	**Silt, %**	**Sand, %**	**Soil Organic Carbon, %**	**Specific Root Length, m/g**
Upper Tucker Prairie	Wockley	29.9576,-95.907	14	19.9	66.1	0.725	102.69
Lower Tucker Prairie	Monaville	29.9523,-95.8999	7.5	6.6	85.9	0.348	102.69
Warren Prairie	Gessner	29.9666,-95.8438	10.5	43.7	45.8	0.725	72.92
Warren Wet Prairie	Gessner	29.9424,-95.8577	10.5	43.7	45.8	0.725	35.3
Upper Tucker Wet Prairie	Nahatche Loam	29.9562,-95.9014	25	36.5	38.5	1.160	75.12
Nelson Rice	Katy	29.9136, 95.8652	10	26.5	63.5	0.725	37.5
Chase North Rice	Katy	29.9091,-95.9284	10	26.5	63.5	0.725	37.5
Warren Millet	Gessner	29.9416,-95.8419	10.5	43.7	45.8	0.725	37.5
Warren Pasture	Hockley	29.9772,-95.8611	14	19.9	66.1	0.725	72.92
Lower Tucker Pasture	Monaville	29.9432,-95.9024	7.5	6.6	85.9	0.348	102.69
Bing	Katy	29.9285,-95.9248	10	26.5	63.5	0.725	72.92
Manor	Katy	29.8963,-95.9033	10	26.5	63.5	0.725	35.3

Clear Creek							
Site name	**Soil Name**	**Location Lat/Long**	**Clay, %**	**Silt, %**	**Sand, %**	**Soil Organic Carbon, %**	**Specific Root Length, m/g**
Grazed Pasture	Gaddy	33.4570,-97.3848	14.0	16.4	69.6	0.15	19.69
Native prairie land	Sanger	33.4403,-97.3986	50	27.9	22.1	1.16	102.69
Ploughed land	Windthorst	33.6545,-97.5689	11.5	21	67.5	0.44	62.5
Rotating grazing/Scotts	Bolar	33.6845,-97.6037	30	36.5	33.5	1.16	61
Grass land	Frio	33.3399,-97.1848	40	52	8	1.45	43.14
Ranch	Medlin	33.3514,-97.2791	50	27.9	22.1	1.16	61
Pasture	Hensley	33.4300,-97.3252	22.5	37.7	39.8	0.73	61
Pasture with rag weed	Bolar	33.4811,-97.4567	30	36.5	33.5	1.16	61
Pasture - Coastal Bermuda grass	Bosque	33.6106,-97.5122	23.5	37.3	39.2	1.45	19.69
Pasture/Oak	Bosque	33.6116,-97.5108	23.5	37.3	39.2	1.45	62.5
Prairie land - Canada wild Rye	Venus	33.6156,-97.5083	24	36.9	39.1	0.87	19.69

APPENDIX B

SATURATED SOIL HYDRAUCLIC OCNDUCTIVITY IN MM/HR FROM CALIBRATION, ESTIMATED FROM RALWS PTF, AND ESTIMATED FROM NEW PTF

CLC			HWC			NTR			UBR		
New_K	Rawls_K	Calibrated_K	New_K	Rawls_K	Calibrated_K	New_K	Rawls_K	Calibrated	New_K	Rawls_K	Calibrated_K
68.48	34.77	25.92	29.65	4.65	24.30	33.70	2.88	10.80	61.88	2.04	19.44
68.48	34.77	32.40	29.65	4.65	24.30	3.83	1.69	10.80	61.88	6.52	64.80
39.61	5.62	32.40	11.09	2.38	24.30	3.83	1.69	2.52	19.82	6.52	64.80
39.61	5.62	32.40	11.09	2.38	24.30	17.79	2.24	2.52	19.82	6.52	64.80
68.48	34.77	25.92	7.50	1.63	2.70	10.17	2.24	10.80	19.82	6.52	64.80
68.48	34.77	25.92	10.63	4.65	24.30	10.17	2.24	10.80	19.82	6.52	64.80
33.43	3.04	100.80	10.63	4.65	24.30	10.17	2.24	2.52	61.88	6.52	64.80
57.30	3.82	100.80	4.75	2.38	24.30	10.96	2.24	2.52	61.88	6.52	64.80
57.30	3.82	32.40	4.75	2.38	24.30	18.57	2.24	10.80	61.88	6.52	64.80
65.08	5.62	32.40	1.24	1.63	5.40	18.57	2.24	10.80	19.82	6.52	64.80
65.08	5.62	32.40	1.24	1.63	5.40	18.57	2.24	10.80	19.82	6.52	64.80
112.45	34.77	32.40	72.26	9.70	24.30	37.38	5.36	10.80	19.82	6.52	64.80
112.45	34.77	32.40	29.65	4.65	24.30	33.70	2.88	10.80	19.82	6.52	64.80
55.25	3.04	32.40	8.13	1.91	8.10	33.70	2.88	10.80	22.82	6.52	64.80
55.25	3.04	32.40	8.13	1.91	8.10	0.94	1.69	10.80	61.88	10.68	64.80
68.48	34.77	100.80	25.77	9.70	24.30	0.94	1.69	10.80	61.88	2.04	19.44
68.48	34.77	100.80	10.63	4.65	24.30	14.24	4.19	2.52	61.88	6.52	64.80
68.48	34.77	32.40	10.63	4.65	24.30	22.60	5.36	2.52	61.88	6.52	64.80
68.48	34.77	32.40	2.85	1.91	8.10	22.60	5.36	10.80	19.82	6.52	64.80
68.48	34.77	32.40	2.85	1.91	8.10	22.60	5.36	10.80	19.82	6.52	64.80
68.48	34.77	32.40	4.75	2.38	24.30	22.60	5.36	10.80	19.82	6.52	64.80
112.45	34.77	100.80	4.75	2.38	24.30	10.66	2.24	10.80	19.82	6.52	64.80
112.45	34.77	100.80	29.65	4.65	24.30	18.28	2.24	10.80	61.88	6.52	64.80
112.45	34.77	32.40	29.65	4.65	24.30	5.87	1.85	10.80	61.88	6.52	64.80
112.45	34.77	32.40	11.58	2.38	24.30	3.24	1.85	10.80	61.88	2.04	19.44
112.45	34.77	32.40	11.58	2.38	24.30	3.24	1.85	10.80	61.88	6.52	64.80
112.45	34.77	32.40	3.62	2.17	24.30	5.87	1.85	32.40	61.88	6.52	64.80
68.48	34.77	100.80	3.62	2.17	24.30	23.25	6.48	10.80	19.82	6.52	64.80

68.48	34.77	100.80	8.08	2.83	24.30	23.25	6.48	10.80	19.82	6.52	64.80
68.48	34.77	32.40	8.08	2.83	24.30	14.03	3.91	2.52	19.82	6.52	64.80
68.48	34.77	32.40	5.24	2.38	24.30	14.03	3.91	2.52	19.82	6.52	64.80
68.48	34.77	32.40	5.24	2.38	24.30	23.95	3.91	32.40	68.25	6.52	64.80
68.48	34.77	32.40	10.63	4.65	24.30	23.68	4.19	32.40	68.25	6.52	64.80
112.45	34.77	100.80	10.63	4.65	24.30	14.24	4.19	32.40	2.29	6.52	64.80
112.45	34.77	100.80	4.75	2.38	24.30	22.60	5.36	32.40	2.29	2.04	19.44
112.45	34.77	32.40	4.75	2.38	24.30	37.38	5.36	32.40	2.29	2.04	19.44
112.45	34.77	32.40	11.09	2.38	24.30	14.03	3.91	10.80	11.26	10.68	64.80
112.45	34.77	32.40	11.09	2.38	24.30	14.03	3.91	10.80	11.26	10.68	64.80
112.45	34.77	32.40	11.58	2.38	24.30	37.38	5.36	10.80	2.64	2.26	64.80
39.61	5.62	32.40	11.58	2.38	24.30	37.38	5.36	10.80	2.64	2.26	64.80
39.61	5.62	32.40	4.75	2.38	24.30	14.03	3.91	10.80	3.87	2.26	64.80
68.48	34.77	32.40	4.75	2.38	24.30	14.03	3.91	10.80	3.87	1.92	66.02
68.48	34.77	32.40	1.64	1.92	24.30	23.95	3.91	32.40	65.79	1.92	66.02
52.93	1.56	9.72	1.64	1.92	24.30	23.36	3.91	32.40	65.79	1.85	66.02
52.93	1.56	9.72	1.64	1.92	24.30	22.60	5.36	32.40	65.79	1.85	66.02
83.82	71.66	100.80	-0.31	4.65	24.30	22.60	5.36	32.40	65.79	1.92	66.02
83.82	71.66	100.80	-0.31	4.65	24.30	22.60	5.36	32.40	2.64	1.92	66.02
68.48	34.77	100.80	0.29	1.82	8.10	14.03	3.91	32.40	3.87	1.85	66.02
68.48	34.77	100.80	1.64	1.92	24.30	14.03	3.91	32.40	2.64	6.48	19.44
39.61	5.62	32.40	1.64	1.92	24.30	23.95	3.91	32.40	2.64	6.48	19.44
39.61	5.62	32.40	1.80	2.51	24.30	34.75	2.88	32.40	11.26	6.48	19.44
52.93	1.56	9.72	1.80	2.51	24.30	23.95	3.91	32.40	11.26	6.48	19.44
52.93	1.56	9.72	-0.31	4.65	24.30	34.75	2.88	32.40	3.87	1.85	66.02
117.44	34.50	100.80	0.29	1.82	8.10	33.89	2.88	32.40	63.61	1.92	66.02
117.44	34.50	100.80	1.60	2.38	24.30	18.74	2.11	32.40	11.39	1.85	66.02
117.44	34.50	100.80	4.67	1.92	24.30	18.74	2.11	32.40	11.26	1.85	66.02
138.62	75.90	100.80	4.67	1.92	24.30	33.70	2.88	32.40	11.26	1.85	66.02
138.62	75.90	100.80	4.67	1.92	24.30	33.70	2.88	32.40	3.87	1.92	66.02
112.45	34.77	32.40	6.05	2.17	24.30	33.70	2.88	32.40	3.87	1.92	66.02
112.45	34.77	32.40	6.05	2.17	24.30	0.94	1.69	32.40	65.79	1.92	66.02
68.48	34.77	100.80	43.60	9.70	24.30	0.94	1.69	32.40	65.79	5.64	66.02
68.48	34.77	100.80	43.60	9.70	24.30	20.21	2.88	32.40	65.79	3.79	64.80
33.43	3.04	25.92	6.63	1.92	24.30	20.21	2.88	32.40	65.79	1.85	66.02
33.43	3.04	25.92	6.63	1.92	24.30	0.94	1.69	32.40	23.73	6.48	19.44

57.30	3.82	32.40	6.63	1.92	24.30	0.94	1.69	32.40	23.73	1.92	66.02
57.30	3.82	32.40	29.65	4.65	24.30	3.48	1.85	10.80	23.73	1.92	66.02
55.25	3.04	25.92	16.94	1.82	8.10	3.48	1.85	32.40	23.73	1.92	66.02
55.25	3.04	25.92	6.51	1.84	8.10	34.56	2.88	10.80	23.73	1.92	66.02
55.25	3.04	25.92	3.46	1.92	24.30	33.70	2.88	10.80	23.73	6.48	19.44
55.25	3.04	25.92	3.46	1.92	24.30	10.17	2.24	10.80	11.26	6.48	19.44
52.93	1.56	9.72	6.37	1.82	8.10	10.17	2.24	10.80	11.26	6.48	19.44
52.93	1.56	9.72	2.28	1.84	8.10	20.21	2.88	10.80	3.87	6.48	19.44
35.94	0.69	0.76	2.28	1.84	8.10	20.21	2.88	10.80	2.64	6.48	19.44
35.94	0.69	0.76	11.58	2.38	24.30	10.66	2.24	10.80	2.64	6.48	19.44
52.93	1.56	9.72	11.58	2.38	24.30	10.66	2.24	10.80	3.87	6.48	19.44
52.93	1.56	9.72	5.24	2.38	24.30	3.48	1.85	10.80	65.79	6.48	19.44
51.22	1.57	9.72	5.24	2.38	24.30	26.08	4.65	32.40	65.79	6.48	19.44
51.22	1.57	9.72	4.75	2.38	24.30	7.45	2.24	32.40	23.73	6.48	19.44
35.94	0.69	0.76	4.75	2.38	24.30	7.27	2.24	32.40	23.73	1.92	66.02
35.94	0.69	0.76	6.05	2.17	24.30	14.03	3.91	32.40	1.99	1.92	66.02
35.45	0.69	0.76	6.05	2.17	24.30	14.03	3.91	32.40			
17.93	1.57	9.72	6.05	2.17	24.30	9.22	2.31	10.80			
17.93	1.57	9.72	13.75	2.83	24.30	9.22	2.31	10.80			
17.93	1.57	9.72	13.75	2.83	24.30	14.04	3.39	32.40			
17.93	1.57	9.72	13.75	2.83	24.30	14.04	3.39	32.40			
12.10	0.69	0.76	13.75	2.83	24.30	14.03	3.91	32.40			
12.10	0.69	0.76	13.75	2.83	24.30	14.03	3.91	32.40			
33.43	3.04	25.92	17.93	4.65	24.30	14.03	3.91	32.40			
33.43	3.04	25.92	17.93	4.65	24.30	7.45	2.24	32.40			
32.41	1.56	9.72	29.65	4.65	24.30	37.38	5.36	32.40			
32.41	1.56	9.72	6.51	1.84	8.10	10.66	2.24	10.80			
39.61	5.62	32.40	6.51	1.84	8.10	10.66	2.24	10.80			
39.61	5.62	32.40	11.58	2.38	24.30	38.88	6.49	32.40			
55.25	3.04	25.92	11.58	2.38	24.30	17.46	2.05	10.80			
55.25	3.04	25.92	3.46	1.92	24.30	17.46	2.05	10.80			
52.93	1.56	9.72	3.46	1.92	24.30	10.15	2.05	10.80			
52.93	1.56	9.72	3.62	2.17	24.30	10.15	2.05	10.80			
35.94	0.69	0.76	3.62	2.17	24.30	10.66	2.24	10.80			
35.94	0.69	0.76	10.63	4.65	24.30	10.66	2.24	10.80			
35.45	0.69	0.76	10.63	4.65	24.30	23.95	3.91	32.40			
35.45	0.69	0.76	5.24	2.38	24.30	17.46	2.05	10.80			
33.43	3.04	25.92	5.24	2.38	24.30	17.46	2.05	10.80			
28.75	1.27	9.72	6.39	1.79	8.10	11.24	2.11	10.80			

28.75	1.27	9.72	6.39	1.79	8.10	11.24	2.11	10.80			
32.41	1.56	9.72	29.65	4.65	24.30	10.15	2.05	10.80			
32.41	1.56	9.72	29.65	4.65	24.30	10.15	2.05	10.80			
39.61	5.62	32.40	6.51	1.84	8.10	10.15	2.05	10.80			
48.03	1.27	9.72	6.51	1.84	8.10	19.43	2.28	10.80			
48.03	1.27	9.72	11.58	2.38	24.30	19.43	2.28	10.80			
52.93	1.56	9.72	11.58	2.38	24.30	39.37	6.48	32.40			
52.93	1.56	9.72	2.16	1.79	8.10	35.69	4.86	32.40			
51.22	1.57	9.72	2.16	1.79	8.10	35.69	4.86	32.40			
51.22	1.57	9.72	2.28	1.84	8.10	0.72	1.85	10.80			
35.94	0.69	0.76	2.28	1.84	8.10	0.72	1.85	10.80			
35.94	0.69	0.76	5.24	2.38	24.30	39.37	6.48	32.40			
33.43	3.04	25.92	5.24	2.38	24.30	34.84	2.92	10.80			
33.43	3.04	25.92	4.67	1.92	24.30	34.84	2.92	10.80			
32.41	1.56	9.72	4.67	1.92	24.30	23.25	6.48	32.40			
32.41	1.56	9.72	4.67	1.92	24.30	23.25	6.48	32.40			
35.24	2.88	32.40	13.75	2.83	24.30	39.37	6.48	32.40			
35.24	2.88	32.40	13.75	2.83	24.30	28.18	1.45	2.52			
39.61	5.62	32.40	13.75	2.83	24.30	37.07	30.67	100.80			
39.61	5.62	32.40	13.75	2.83	24.30	37.07	30.67	100.80			
52.93	1.56	9.72	13.75	2.83	24.30	39.37	6.48	32.40			
52.93	1.56	9.72	17.93	4.65	24.30	34.52	4.87	32.40			
33.43	3.04	25.92	17.93	4.65	24.30	37.07	30.67	100.80			
33.43	3.04	25.92	5.09	1.83	7.29	37.07	30.67	100.80			
28.75	1.27	9.72	5.09	1.83	7.29	11.21	2.75	32.40			
28.75	1.27	9.72	29.65	4.65	24.30	34.84	2.92	10.80			
32.41	1.56	9.72	11.58	2.38	24.30	28.18	1.45	2.52			
32.41	1.56	9.72	11.58	2.38	24.30	35.69	4.86	32.40			
39.61	5.62	32.40	11.58	2.38	24.30	35.69	4.86	32.40			
55.25	3.04	25.92	11.58	2.38	24.30	0.00	4.86	32.40			
55.25	3.04	25.92	3.46	1.92	24.30	0.00	4.86	32.40			
48.03	1.27	9.72	3.46	1.92	24.30	21.18	6.48	32.40			
48.03	1.27	9.72	2.28	1.84	8.10	21.18	1.45	2.52			
48.03	1.27	9.72	2.28	1.84	8.10	39.37	1.45	2.52			
52.93	1.56	9.72	5.24	2.38	24.30	28.18	1.45	2.52			
52.93	1.56	9.72	5.24	2.38	24.30	16.87	1.45	2.52			
34.70	3.82	32.40	13.45	2.51	24.30	16.87	2.92	10.80			
34.70	3.82	32.40	13.45	2.51	24.30	28.91	1.45	2.52			
21.05	0.69	3.60	29.65	4.65	24.30	34.84	3.91	32.40			

21.05	0.69	3.60	6.51	1.84	8.10	28.18	3.91	32.40			
57.30	3.82	32.40	6.51	1.84	8.10	14.03	3.91	32.40			
57.30	3.82	32.40	11.58	2.38	24.30	14.03	2.75	32.40			
35.94	0.69	0.76	11.58	2.38	24.30	14.03	2.75	32.40			
35.94	0.69	0.76	6.06	2.51	24.30	6.63	8.11	32.40			
59.15	3.17	32.40	6.06	2.51	24.30	6.63	8.11	32.40			
59.15	3.17	32.40	2.28	1.84	8.10	24.57	8.11	32.40			
35.94	0.69	0.76	2.28	1.84	8.10	24.57	30.67	100.80			
35.94	0.69	0.76	5.24	2.38	24.30	24.57	2.92	10.80			
35.94	0.69	0.76	5.24	2.38	24.30	62.39	2.92	10.80			
35.94	0.69	0.76	6.51	1.84	8.10	35.73	1.45	2.52			
35.94	0.69	0.76	6.51	1.84	8.10	34.84	30.67	100.80			
59.15	3.17	32.40	11.58	2.38	24.30	28.18	30.67	100.80			
59.15	3.17	32.40	11.58	2.38	24.30	37.07	1.45	2.52			
12.59	0.69	0.76	3.46	1.92	24.30	37.07	1.45	2.52			
12.59	0.69	0.76	3.46	1.92	24.30	16.87	4.87	32.40			
12.59	0.69	0.76	2.28	1.84	8.10	28.91	1.45	2.52			
12.10	0.69	0.76	2.28	1.84	8.10	34.52	3.40	32.40			
21.22	3.17	32.40	5.24	2.38	24.30	28.18	3.40	32.40			
21.22	3.17	32.40	5.24	2.38	24.30	13.06	2.88	10.80			
52.93	1.56	9.72				13.06	2.88	10.80			
52.93	1.56	9.72				20.41	2.88	10.80			
35.45	0.69	0.76				20.41	2.06	10.80			
55.25	3.04	25.92				20.41	2.06	10.80			
55.25	3.04	25.92				10.24					
17.93	1.57	9.72				10.24					
17.93	1.57	9.72									
12.10	0.69	0.76									
12.10	0.69	0.76									
52.93	1.56	9.72									
52.93	1.56	9.72									
51.22	1.57	9.72									
51.22	1.57	9.72									
51.22	1.57	9.72									
55.25	3.04	32.40									
55.25	3.04	32.40									
35.45	0.69	0.76									
55.25	3.04	25.92									
55.25	3.04	25.92									

55.25	3.04	32.40									
55.25	3.04	32.40									
35.45	0.69	0.76									
17.93	1.57	9.72									
17.93	1.57	9.72									
19.86	3.04	32.40									
19.86	3.04	32.40									
12.10	0.69	0.76									
12.10	0.69	0.76									
35.94	0.69	0.76									
35.94	0.69	0.76									
35.94	0.69	0.76									
35.94	0.69	0.76									
59.15	3.17	32.40									
59.15	3.17	32.40									
66.97	15.36	32.40									
66.97	15.36	32.40									
66.97	15.36	32.40									
7.73	1.60	9.72									
7.73	1.60	9.72									
7.73	1.60	9.72									
35.77	3.17	32.40									
35.77	3.17	32.40									
35.77	3.17	32.40									
116.10	30.94	100.80									
116.10	30.94	100.80									
12.94	1.60	9.72									
12.94	1.60	9.72									
12.94	1.60	9.72									
60.51	3.65	9.72									
60.51	3.65	9.72									
35.94	0.69	0.76									
35.94	0.69	0.76									
35.94	0.69	0.76									
59.15	3.17	32.40									
59.15	3.17	32.40									
57.30	3.82	32.40									
57.30	3.82	32.40									

116.10	30.94	100.80									
116.10	30.94	100.80									
35.94	0.69	0.76									
35.94	0.69	0.76									
40.19	15.36	32.40									
4.49	1.60	9.72									
4.49	1.60	9.72									
21.22	3.17	32.40									
34.70	3.82	32.40									
34.70	3.82	32.40									
34.70	3.82	32.40									
66.97	15.36	32.40									
66.97	15.36	32.40									
66.97	15.36	32.40									
7.73	1.60	9.72									
7.73	1.60	9.72									
66.52	6.47	9.72									
66.52	6.47	9.72									
57.30	3.82	32.40									
57.30	3.82	32.40									
55.25	3.04	25.92									
55.25	3.04	25.92									
55.25	3.04	25.92									
48.03	1.27	9.72									
48.03	1.27	9.72									
57.30	3.82	32.40									
57.30	3.82	32.40									
110.03	15.36	32.40									
110.03	15.36	32.40									
110.03	15.36	32.40									
57.30	3.82	32.40									
57.30	3.82	32.40									
35.94	0.69	0.76									
35.94	0.69	0.76									
35.94	0.69	0.76									
35.94	0.69	0.76									
59.15	3.17	32.40									
59.15	3.17	32.40									

12.94	1.60	9.72									
12.94	1.60	9.72									
35.94	0.69	0.76									
35.94	0.69	0.76									
35.94	0.69	0.76									
35.94	0.69	0.76									
59.15	3.17	32.40									
59.15	3.17	32.40									
35.45	0.69	0.76									
35.45	0.69	0.76									
59.15	3.17	32.40									
59.15	3.17	32.40									
35.45	0.69	0.76									
35.45	0.69	0.76									
35.45	0.69	0.76									
35.94	0.69	0.76									
35.94	0.69	0.76									
59.15	3.17	32.40									
59.15	3.17	32.40									
35.45	0.69	0.76									
35.45	0.69	0.76									
35.45	0.69	0.76									
35.45	0.69	0.76									
35.94	0.69	0.76									
35.94	0.69	0.76									
12.10	0.69	0.76									
12.10	0.69	0.76									
-0.38	1.60	9.72									
-0.38	1.60	9.72									
-0.38	1.60	9.72									
-0.62	2.88	32.40									
-0.62	2.88	32.40									
-0.62	2.88	32.40									
7.73	1.60	9.72									
7.73	1.60	9.72									
12.94	1.60	9.72									
12.94	1.60	9.72									
12.94	1.60	9.72									
58.30	2.88	32.40									

58.30	2.88	32.40									
35.94	0.69	0.76									
35.94	0.69	0.76									
59.15	3.17	32.40									
59.15	3.17	32.40									
57.30	3.82	32.40									
57.30	3.82	32.40									
35.94	0.69	0.76									
35.94	0.69	0.76									
59.15	3.17	32.40									
59.15	3.17	32.40									
59.15	3.2	32.4									